Electrochemical Energy Reviews (2020) 3:690–729
https://doi.org/10.1007/s41918-020-00077-0

REVIEW ARTICLE

Electrochemical Compression Technologies for High-Pressure Hydrogen: Current Status, Challenges and Perspective

Jiexin Zou[1,2] · Ning Han[2,5] · Jiangyan Yan[2,3] · Qi Feng[1,4] · Yajun Wang[1,2] · Zhiliang Zhao[4] · Jiantao Fan[4] · Lin Zeng[2] · Hui Li[4] · Haijiang Wang[2,4]

Received: 6 January 2020 / Revised: 14 April 2020 / Accepted: 8 July 2020 / Published online: 7 August 2020

Abstract

Hydrogen is an ideal energy carrier in future applications due to clean byproducts and high efficiency. However, many challenges remain in the application of hydrogen, including hydrogen production, delivery, storage and conversion. In terms of hydrogen storage, two compression modes (mechanical and non-mechanical compressors) are generally used to increase volume density in which mechanical compressors with several classifications including reciprocating piston compressors, hydrogen diaphragm compressors and ionic liquid compressors produce significant noise and vibration and are expensive and inefficient. Alternatively, non-mechanical compressors are faced with issues involving large-volume requirements, slow reaction kinetics and the need for special thermal control systems, all of which limit large-scale development. As a result, modular, safe, inexpensive and efficient methods for hydrogen storage are urgently needed. And because electrochemical hydrogen compressors (EHCs) are modular, highly efficient and possess hydrogen purification functions with no moving parts, they are becoming increasingly prominent. Based on all of this and for the first time, this review will provide an overview of various hydrogen compression technologies and discuss corresponding structures, principles, advantages and limitations. This review will also comprehensively present the recent progress and existing issues of EHCs and future hydrogen compression techniques as well as corresponding containment membranes, catalysts, gas diffusion layers and flow fields. Furthermore, engineering perspectives are discussed to further enhance the performance of EHCs in terms of the thermal management, water management and the testing protocol of EHC stacks. Overall, the deeper understanding of potential relationships between performance and component design in EHCs as presented in this review can guide the future development of anticipated EHCs.

Keywords Hydrogen storage · Hydrogen energy · Non-mechanical compressor · Electrochemical hydrogen compressor · Purification function

✉ Lin Zeng
zengl3@sustech.edu.cn

✉ Hui Li
hui.li@sustech.edu.cn

✉ Haijiang Wang
wanghj@sustech.edu.cn

[1] School of Mechanical Engineering, Harbin Institute of Technology, Harbin 150001, Heilongjiang, China

[2] Department of Mechanical and Energy Engineering, Southern University of Science and Technology, Shenzhen 518055, Guangdong, China

[3] Department of Power Engineering, Wuhan University, Wuhan 430072, Hubei, China

[4] Department of Materials Science and Engineering, Shenzhen Key Laboratory of Hydrogen Energy, Shenzhen Clean Energy Research Institute, Southern University of Science and Technology, Shenzhen 518055, Guangdong, China

[5] Department of Materials Engineering, Katholieke Universiteit Leuven, 3001 Leuven, Belgium

1 Introduction

Although energy is a significant vector in modern society, the unrestrained use of fossil fuels in the past few centuries has led to energy shortages along with global warming, air pollution and other environmental concerns. To address these issues, the development of novel renewable energy technologies with abundant resources, wide distributions, renewability and environmental friendliness has become the best choice to reduce fossil fuel consumption. And although current research has been focused on new energy technologies based on wind energy, tide energy and solar energy [1], the large-scale application of these new energy technologies is hindered by intrinsic unpredictability and intermittency [2]. Therefore, the search for novel energy carriers that can enable transfer between renewable resources and end-use customers is vital. Here, hydrogen as a completely pollution-free, carbon–neutral energy carrier is extremely promising in the addressing of these issues.

Hydrogen as a carbon-free fuel produces only water in related processes in which a carbon-free cycle is formed through the generation of water and hydrogen with clean and abundant energy. Hydrogen as an energy vector can also play an important role in society in which at the consumer or end-customer level, approximately three-quarters of primary energy is used as fuel and one-quarter is used as electricity [3]. Based on this, primary energy sources must be transformed into energy carriers for consumers. Here, hydrogen is a versatile primary energy source that can be converted into other forms of energy through five different approaches, including flame combustion, direct steam production, catalyst combustion [4], chemical reaction (hydrating) [5] and electrochemical conversion (fuel cells) [6]. In addition, based on the conversion efficiency of hydrogen into thermal, mechanical and electrical forms, it is more efficient to convert hydrogen into desired energy forms than other fuels [7]. Moreover, hydrogen also possesses an attractively high energy density between 120 MJ kg^{-1} (the lower heating value, LHV) and 142 MJ kg^{-1} (the higher heating value, HHV) [8] and has shown great promise in many fields. In terms of industrial application, hydrogen is primarily used as a reactant in fertilizer production and as a refinement material for metal processing [9]. Moreover, hydrogen is being increasingly used as a fuel in hydrogen refueling stations (HRSs) and proton exchange membrane fuel cells (PEMFCs) [10].

However, the promotion of hydrogen still faces a series of challenges, including production, storage and transportation. For hydrogen production, most industrial hydrogen is currently produced from fossil fuels through partial oxidation, autothermal oxidation, steam reforming and gasification [11] in which hydrogen from steam reforming suffers from serious issues (i.e., large numbers of impurities such as carbon monoxide) that need to be resolved before use. Hydrogen storage technologies are also limited by several issues, including low volume energy density, low efficiency compression and high-cost pressure vessels. And due to low-volume densities, hydrogen storage also requires high-pressure vessels or liquefication under low temperatures in which due to bulky storage tanks, most hydrogen storage systems can only be used in stationary applications. As for hydrogen transport, industrial standards in the large-scale use of hydrogen require airtight shipping containers, the transport and storage of which can lead to further cost increases in hydrogen systems [12].

One key technology for the advancement of hydrogen technology application is hydrogen storage in which ideal storage technologies require: (1) reversible storage, (2) high efficiency, (3) high gravimetric and volumetric energy densities, (4) enhanced safety and (5) cost-effectiveness. Here, common technologies used for increasing the volumetric energy density of hydrogen involve compression and liquefaction. For liquefaction, the critical liquefaction process (temperature of − 252.882 °C and pressure of 1.298 MPa) is an energy-intensive process that requires the use of cryogenic refrigeration to compress gaseous hydrogen into liquid hydrogen [13]. Alternative to the harsh requirements of liquefaction, direct compression is a more economical and convenient process in which associated hydrogen compressors are important for the development of hydrogen energy industry. Here, two main methods exist for the direct compression of hydrogen which are mechanical and non-mechanical methods. And although the use of mechanical compressors is the most conventional method, it is accompanied by several disadvantages. First, mechanical compressors possess lower efficiency in terms of the adiabatic compression process as compared with isothermal compression under the same compression ratios. Second, the moving parts of mechanical compressors can easily be damaged due to harsh operating conditions (huge pressure and low temperature) [14] and last, mechanical compressors are noisy due to vulnerable moving parts in which the US department of energy (DOE) reported that hydrogen compressors were the second most problematic component in HRSs to account for 18% of total incidents and a model designed by the national renewable energy laboratory (NREL) showed that compression accounted for the largest percentage of HRS operating costs (Fig. 1a) [15].

In terms of non-mechanical compressors, the absence of moving parts with the reduction in noise is an obvious advantage that can not only reduce the possibility of compressor failure to deliver cost savings but also improve the safety of devices. Currently, non-mechanical hydrogen compressors include cryogenic compressors, adsorption compressors, metal hydride compressors and electrochemical hydrogen compressors (EHCs) and with the exception of modular EHCs, all require large-scale sites. And because

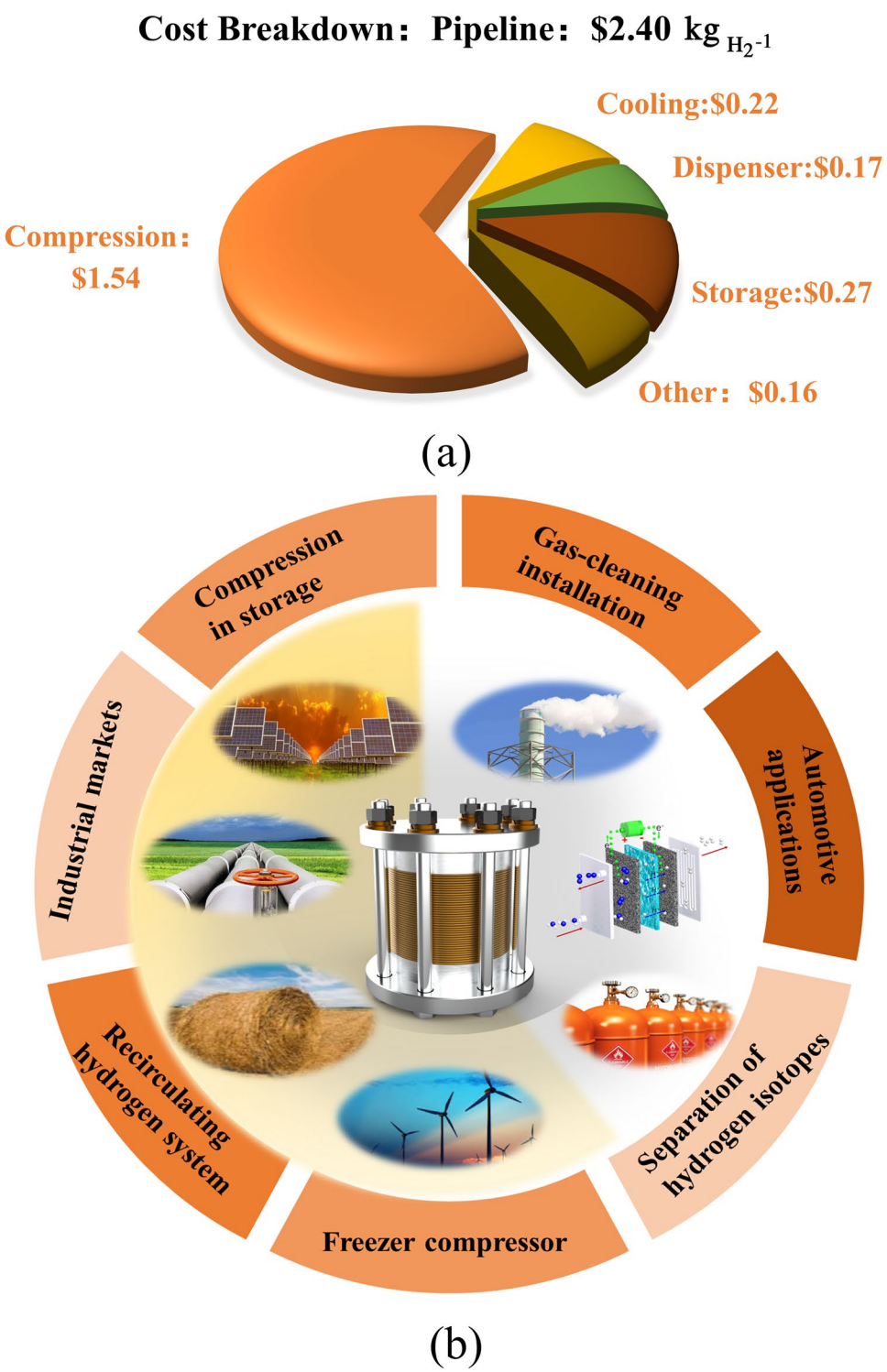

Fig. 1 (**a**) Cost breakdown of the NREL hydrogen delivery scenario analysis mode-pipeline scenario; (**b**) schematic showing the relationship between EHCs, renewable energy sources (solar, wind, biomass), fossil fuels (reforming gas), natural gas transportation and hydrogen demand in industrial markets, including energy storage and automotive applications using hydrogen as a carrier

EHCs can allow for the electrochemical compression of hydrogen with lower electric power consumption, reduced thermal loss and higher efficiency as compared with other non-mechanical hydrogen compressors as well as simple device designs, they have attracted significant attention in the last decade. In addition, the low-pressure requirements at the initial input of EHCs for the storage of hydrogen can reduce safety risks and EHCs can allow for the simultaneous compression and purification of gaseous hydrogen, making EHCs one of the most promising choices for hydrogen compression in the future.

More importantly, the electricity consumed by EHCs during operation can be supplied from surplus solar, wind or biomass energy and low-pressure hydrogen can be

supplied from hydrogen reforming, electro-water splitting or hydrogen storage. Furthermore, the outlet high-pressure and pure hydrogen from EHCs can be directly input into various applications including industry, storage and automobile applications. And as a result of these advantages, EHCs can also be applied in anodes because a recirculating hydrogen system can reduce the frequency of purging operations and voltage pulsations to result in higher efficiency [16, 17] in which Barbir et al. [18] in 2006 evaluated the use of EHCs for the recirculation of hydrogen in a 10-cell EHC and achieved satisfactory and stable results. More recently, many projects based on EHCs have been developed for freezer compressors [19], infrared detectors in aerospace applications [20], gas-cleaning installations [21], etc. and other studies have explored the industrial-scale separation of hydrogen isotopes based on EHCs (Fig. 1b) [22].

Based on all of this and to guide the further development of EHCs, this review will first briefly introduce the operational principles and characteristics of all hydrogen compressors followed by the emphasis of EHC principles and their significant potential for real-world application. Subsequently, this review will analyze the basics of EHC operating procedures and levels of performance along with technologies and design features potentially achievable. More specifically, this review will discuss the current components of EHCs with a focus on technological limitations and current performances and outline existing methods for performance improvements.

2 Hydrogen Compression Technologies

In general, hydrogen compressors can be divided into mechanical and non-mechanical compressors [23], and in this section, both compressors along with their advantages and disadvantages are introduced with a focus on EHCs.

2.1 Mechanical Hydrogen Compressor

Mechanical compressors are the most widely used compressors to compress low-pressure hydrogen into high-pressure tanks by using mechanical energy in which with the lowering of confined volume, gaseous hydrogen can be squeezed into smaller chambers and result in higher gas pressures. In the following sections, general mechanical compressors including reciprocating piston compressors, hydrogen diaphragm compressors and ionic liquid compressors will be briefly introduced.

2.1.1 Reciprocating Piston Compressor

One example of mechanical compressors is the reciprocating piston compressor which is equipped with two separate automatic valves for inlet and outlet hydrogen, and a piston-cylinder system constitutes a single-stage reciprocating compressor (Fig. 2a). Here, a connecting rod connects a piston to a crankshaft and the piston transforms the rotary motion of a moving unit into the approximate linear motion of the piston. This movement is referred to as reciprocating motion [24] in which specifically, the piston moves forth and back in a cylinder to compress hydrogen gas with its head. In most applications, this sequence of movements is driven by a pump that is connected to two cylinders in which the compression step follows an expansion step, which comprises the working principle of reciprocating piston compressors. Overall, reciprocating compression is a mature technology that can be used to compress almost all gases and high-pressure hydrogen can be obtained by using reciprocating compressors with multi-stage configurations. Because of this, reciprocating compressors can provide flexibility during compression. Despite this, reciprocating compressors also possess several limitations that hinder application in hydrogen compression. As one disadvantage, the durability of compressor components is affected by the use of lubricants and can lead to risks of explosion, meaning oil-free compressors are preferred [25]. The presence of moving parts can also lead to increased costs due to manufacturing complexities and difficulties as well as increased maintenance frequencies during operation. Moreover, moving parts also generate heat and decrease the efficiency of overall systems [26]. Furthermore, the reciprocating process of pistons can cause pressure fluctuations that can lead to vibrations, noise and even disastrous explosions [27]. Reciprocating compressors are also not efficient at high flow rates despite high flow rates being potentially achievable [28] depending on the number of cycles and the dimension of cylinders in which in addition to the weight of minimum mechanical compressors being normally heavy (200–400 kg), increases to cylinder dimensions can further lead to bulkier systems that can in turn increase internal forces. And in order to reduce the influence of mechanical stress, lower speeds are preferred, meaning that high-compression speeds can only be achieved in the small scale, which restricts allowable flow rates.

As for industrial application, reciprocating piston compressors may be a good solution for large-scale mechanical compressors used in HRSs in which many projects can attain high-compression levels up to 70 MPa and 85 MPa through multi-stage compression. In addition, outlet pressures of 100 MPa and flow capacities of 300 N m^3 h^{-1} have been attained in a Hitachi infrastructure system [29].

2.1.2 Diaphragm Compressor

Diaphragm compressors follow a similar working principle to reciprocating piston compressors in which with pistons pulling downwards, hydraulic oil can flow back to the

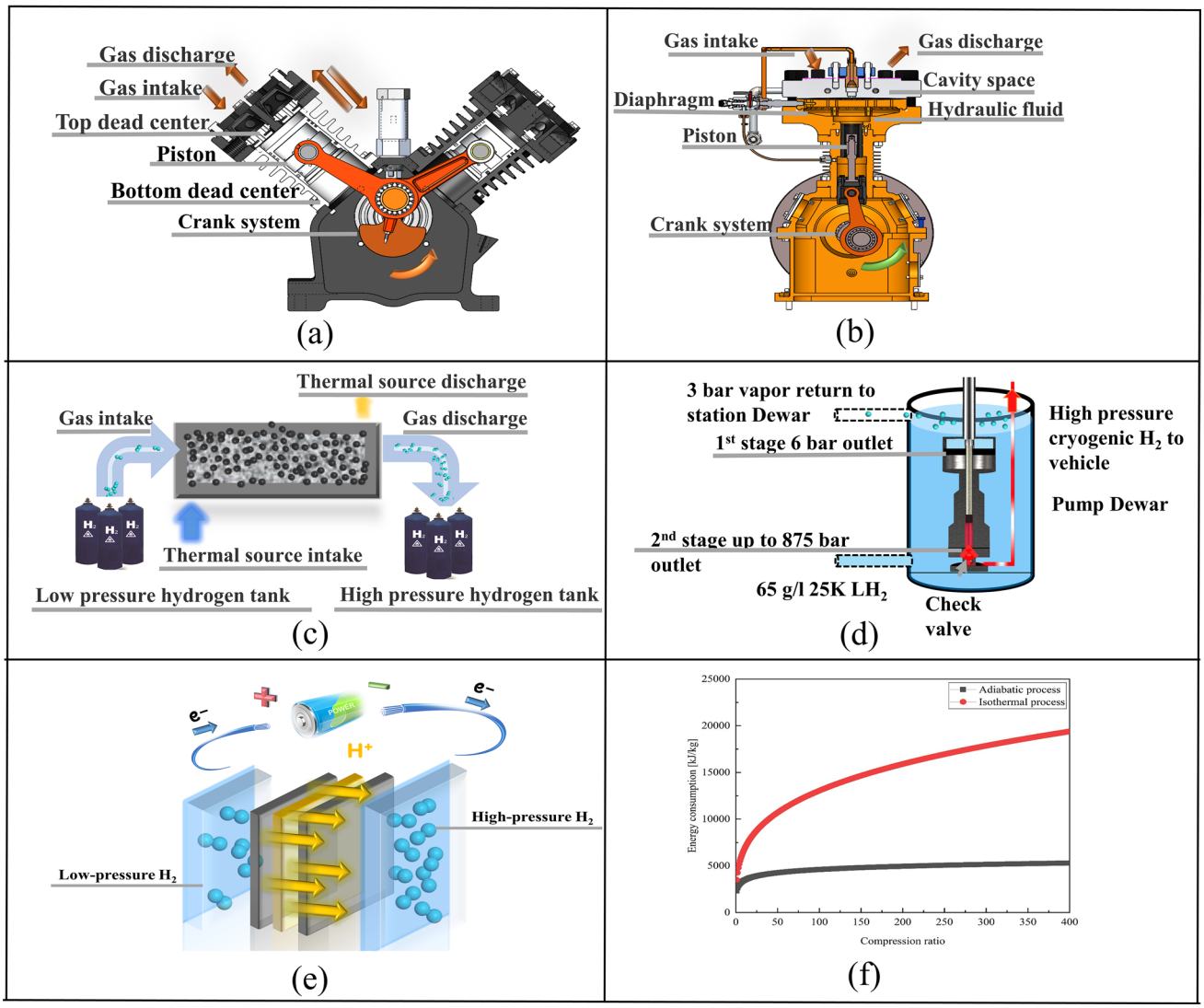

Fig. 2 (**a**) Schematic of a reciprocating piston compressor; (**b**) schematic of a diaphragm compressor; (**c**) schematic of a cryogenic compressor; (**d**) schematic of an adsorption compressor; (**e**) schematic of an electrochemical hydrogen compressor; (**f**) energy compression in adiabatic and isothermal processes

cylinder. Here, the resulting differential pressure can cause the downward elastic deformation of a diaphragm to increase the volume of a corresponding chamber and automatically open a gas inlet valve to suck gas in. Alternatively, as a con-rod pushes the piston upward, the piston will further push the hydraulic oil to cause the upward elastic deformation of the diaphragm (Fig. 2b) and decrease the volume of the gas chamber to result in hydrogen compression. And as gas pressures reach a certain level, a gas discharge valve will open automatically [30]. Based on this mechanism, diaphragm compressors possess lower-power consumption, high throughput and cooling requirements and therefore are considered to be effective for hydrogen compression [31]. In addition, diaphragm compressors also possess the potential to achieve high levels of volumetric efficiency, which further demonstrates its energy-saving advantages [32]. Despite this, the durability of diaphragm compressors is a critical issue in which reciprocating parts can easily be broken by mechanical stress during operation. And similar to reciprocating piston compressors, diaphragm compressors also possess relatively complex operating systems that are more suitable for applications requiring low flow rates in limited volume compression chambers [33]. Moreover, diaphragm failure can also occur as caused by radial stress related to diaphragm deflection [34] and the geometric design of cavity spaces. And because high flow rates can invalidate diaphragms, corresponding concavities and grooves need to be properly designed to ensure proper flow distribution. As a result, new designs for diaphragm plates are based on numerical simulation models [35, 36].

As for current diaphragm compressor applications, a German company named Hofer that is well-known for its hydrogen diaphragm compressor has equipped several HRS systems with diaphragm compressor to compress gases at ~ 390–581 N m^3 h^{-1} with discharge pressures up to 28.1 MPa [37]. In addition, PDC machines have developed products to operate at discharge pressures ranging from 48.2 to 103.4 MPa with production rates ranging from 5 to 2500 kg daily [38, 39]. The Arizona Public Service company also built a three-stage diaphragm compressor that is capable of compressing hydrogen up to 41 MPa in a hydrogen and natural gas fueling station in downtown Phoenix [40].

2.1.3 Ionic Liquid Compressor

Ionic liquid compressors are also based on the same operating principles as reciprocating compressors. In the designed structure, solid pistons are replaced by ionic liquids in which ionic liquids are directly pumped into the compression chamber/chambers to compress hydrogen and send it back to the hydraulic system afterward [41]. Here, researchers have shown that the replacement of hydraulic oil with appropriate ionic liquids in a compressor can contribute to remarkable improvements in volumetric efficiency of approximately 10%–30% [42]. In addition, Kermani et al. [43] found that two imidazolium-based ionic liquids, [EMIM][Tf_2N] and [EMIM][CF_3SO_3], with significantly lower viscosity and corrosion current densities for AISI 316L can demonstrate desirable performances in ionic liquid hydrogen compressors. Moreover, Linde, a German international company, was able to develop a ionic liquid compressor with only eight moving units for hydrogen applications [44].

The fewer moving parts of ionic liquid compressors can further lead to the reduction in mechanical loss and the improvement in overall efficiency for hydrogen compression. And due to the unique properties of ionic liquids, especially their insolubility with gases, many complex designs involving bearings and sealings have been removed to significantly reduce overall system complexities. In addition, the reduction in mechanical parts can also significantly decrease operational expenses and extend the mechanical life in which the service life of ionic liquid compressors is almost ten times longer than that of regular reciprocating compressors. Furthermore, ionic liquid compressors can compress hydrogen gas to 90 MPa in five steps and the removal of lubricating oils allows for extremely pure hydrogen. Moreover, the ionic liquids used in these compressors display good coolant properties and lubricating performances. Overall, ionic liquid compressors are designed especially for increased hydrogen compression efficiency with ionic liquids possessing good chemical and thermal stability, enhanced fire retardance, high ionic conductivity, high polarity, negligible volatility and moderate viscosity [45]. Ionic liquids are also non-toxic and possess low compressibility, low volatility and good lubricating performances, especially for high-pressure applications [46, 47].

Despite these desirable attributes, ionic liquid compressors are not perfect and possess obvious drawbacks, such as the risk of corrosion, the possibility of leakage and the complexity of system design. In addition, ionic liquids can leave compression chambers through discharge tubes with small amounts of hydrogen, resulting in the need for additional cleaning processes for outlet hydrogen [48].

In terms of real-world application, the Linda Group has developed an ionic liquid compressor that can achieve compression pressures up to 45–90 MPa with a net capacity of 8–30 kg h^{-1} [44]. Nasrin has also designed a hydraulic to pneumatic transformer to integrate pneumatic and hydraulic systems for an ionic liquid compressor that can build high pressures above 70 MPa [49].

2.2 Non-mechanical Hydrogen Compressor

Despite the widespread adoption of mechanical compressors, many problems exist. Based on this, other types of compressors with non-mechanical principles have been developed, including cryogenic compressors, adsorption compressors, metal hydride compressors and EHCs. In this section, the general principles and features of these non-mechanical hydrogen compressors are introduced.

2.2.1 Cryogenic Compressor

In general, several modular elements make up a cryogenic compressor, including a container for low-pressure liquid hydrogen storage, a cryogenic compression container and a cryogenic pump in which liquid hydrogen is fed into a cryogenic pump through a vacuum-insulated tube and stabilized to a desired pressure through a cryogenic compressor (Fig. 2c) [50]. Vaporizers are also placed downstream of cryogenic pumps to ensure the acquisition of high-pressure hydrogen [51]. Here, cryogenic compressors can attain higher (more than two times) volumetric efficiency than mechanical compressors [52] and compressed hydrogen possesses high hydrogen densities, meaning cryogenic compressors possess high gravimetric and volumetric capacities and are suitable for large-scale hydrogen storage and compression.

Despite these advantages, hydrogen cryogenic compressors also possess an obvious drawback involving the energy cost that is a critical barrier hindering future application in which of total input energy, only 30% is stored based on the lowered heating value of hydrogen. The storage of liquefied hydrogen is also an issue hindering application due to the

difficulty in ensuring long-term vacuum stability for about 10 years. And although the high-temperature baking of metal surfaces can increase the degree of vacuum stability in internal pressure vessels made of composite materials [53], it poses great challenges in the rational design of materials and the investigation of compressor fabrication methods.

As for industrial applications, a cryogenic compressor manufactured by the Linda Group company used in hydrogen refueling stations can reach pressures up to 35–90 MPa with high throughput (100 kg h^{-1}, enough to fill an automobile in 5 min). In addition, the benefits of cryogenic container technologies have been comprehensively evaluated by establishing a method to evaluate the filling density in any initial thermodynamic state of containers [50] and Kunze et al. [54] introduced a cryogenic compressor that can compress hydrogen up to 30 MPa. Despite this, many problems exist in the development of cryogenic compressors that need to be conquered before industrial application [55, 56].

2.2.2 Adsorption Compressor

In terms of adsorption compressors, corresponding structures can be seen as a thermodynamic engine by using heat exchange as the driving force of compression (Fig. 2d) in which low-pressure hydrogen is injected into high-adsorption potential porous materials in a compressor, and physical hydrogen adsorption is desorbed at a certain volume after reaching high pressures under specific temperature and pressure conditions [57]. And depending on the physical nature of porous materials, the flow of compressed hydrogen is obtained through multiple cycles of adsorption/desorption.

Adsorption compressors have been widely used as hydrogen compressors due to several advantages. Not only do adsorption compressors require less pressure to store hydrogen and enhance safety, but these compressors also do not possess any moving parts and therefore do not generate noise or experience mechanical damage. In addition, more hydrogen can be obtained through the use of porous materials per unit volume as compared with mechanical compressors [58] in which zeolites, carbonaceous materials (i.e., activated carbons, carbon nanotubes or fullerenes) and metal–organic frameworks (MOFs) are usually used as porous materials in adsorption compressors [59, 60]. Here, the interaction between hydrogen and solid bed surfaces through weak Van der Waals forces can drive the formation of monolayered hydrogen molecules on absorbent surfaces. Moreover, required adsorbent materials in adsorption compressors are readily available and the driven forces of industrial waste heat can be used to lower system costs.

Adsorption compressors possess weaknesses as well, especially due to issues concerning heat and mass transfer in adsorbent beds, leading to the need for cooling systems and increased complexity in overall systems [61]. In addition, because the cycling of adsorption and desorption in adsorption compressors is intermittent in nature, adsorbent beds experience thermal gradient differences that can affect operating efficiency [62]. Moreover, the need for high vacuum conditions also creates technical engineering problems which if not evaluated properly, adsorption heat would increase temperatures and reduce adsorption capacity and system performance [63]. Furthermore, because the heat energy of hydrogen molecules is directly proportional to the temperature of the system [64], the interactions between adsorbent surfaces and gas molecules can increase with cooling systems. However, the adsorption of hydrogen usually occurs at reaction temperatures (~ 77 K) that are too low.

Despite these issues, adsorption compressors have proven to be an appropriate choice for industrial hydrogen compression. For example, various prototypes [65, 66] have demonstrated high-efficiency compression capabilities in which through the use of activated carbon as an adsorbent material, hydrogen with a pressure of 10 MPa can be obtained. Richard et al. [67] also used Maxsorb MSC-30TM-activated carbon as an adsorbent material to successfully compress hydrogen from 0.25 to 35 MPa. Based on these results, new technologies for adsorption compressors should be further developed.

2.2.3 Metal Hydride Compressor

As for metal hydride compressors (MHCs), they are made up of a slender central artery to distribute hydrogen inside a reactor and an annular space between the artery and a tank wall for metal hydride placement. In principle, low-pressure hydrogen can enter the metal hydride tank through the central artery and diffuse into the metal hydride bed to allow for the exothermic reaction of hydrogen absorption in which hydrogen compression can occur due to the continuous cooling and heating of the metal hydride as controlled by heat transfer [68]. Here, the selection of well-suited metal hydrides with BCC, AB_5 and AB_2 structures is vital [69] in which Ni-based AB_5 hydrides have been found to be particularly promising due to their low costs and acceptable performances, especially at moderate temperatures.

In terms of advantages, MHCs possess straightforward designs with no moving parts and can operate with no noise and are not energy intensive. In addition, MHCs are also more compact and can more easily integrate into existing hydrogen refueling infrastructures [70]. Furthermore, MHC systems can be powered by using industrial waste heat rather than electricity in which high-pressure hydrogen can be obtained in situ from water through connections with electrolytic cell outlets to recover heat loss from electrolysis [71].

Unfortunately, the efficiency of MHCs is generally less than 25% at 423 K [69] and strictly depends on the compression rate and the amount of heat provided to the system due to several types of energy loss, including heat transfer as well as heat for hydrogen desorption and cooling. Furthermore, the use of MHCs results in large volumes, slow refueling times and low gravimetric densities and therefore is unsuitable for small mobile power stations. Moreover, the durability of MHCs is still currently unsatisfactory.

As for practical application, many MHCs have been developed with outlet pressures up to 35–70 MPa [72, 73]. For example, Pickering et al. [74] reported promising hydrogen absorption capacities in vanadium-based BCC solid solution alloys with high absorption/desorption kinetics at ambient temperature in which the addition of small amounts of niobium and manganese to Ti–V based alloys can result in a pressure of 65 MPa at moderate temperatures.

2.2.4 Electrochemical Hydrogen Compressor

Electrochemical hydrogen compressors (EHCs) are devices that use the electrochemical principle to compress low-pressure hydrogen into high-pressure hydrogen in which the application of voltage can lead to the generation of localized pressure difference due to hydrogen oxidation at anodes and hydrogen reduction at cathodes. Here, protons and electrons produced through hydrogen oxidation are transported to the cathode side through a proton exchange membrane (PEM) (for protons) and an external path (for electrons) to recombine to form new hydrogen molecules (Fig. 2e) in which electric power is converted to chemical potential in high-pressure hydrogen gas through the electrochemical process. As a result, EHC systems are analogous to proton exchange membrane fuel cells (PEMFCs) and contain PEMs, catalyst layers (CLs), gas diffusion layers (GDLs), flow field plates and end plates.

Overall, ideal compression should be isothermal in nature and operate without heat generation as shown in Eq. (1) as dictated through thermodynamic principles [the energy needed for the adiabatic process in mechanical compressors is expressed in Eq. (2) for comparison]:

$$W = RT\ln\left(\frac{P_c}{P_a}\right) \tag{1}$$

$$W = \frac{\gamma}{\gamma - 1}RT\left[\frac{P_c^{(\gamma-1)/\gamma}}{P_a}\right] \tag{2}$$

in which W represents power required for compression, R is the gas constant of 8.314 J mol^{-1} K^{-1}), γ is the ratio of specific heat (for H_2, γ is 1.4), P_c and P_a represent hydrogen pressure at high-pressure and low-pressure sides, respectively, and T represents the temperature of hydrogen on the low-pressure side. Based on these equations, it can be seen that the theoretical efficiency of isothermal compression is almost two times higher than that of adiabatic compression with a compression ratio of 300 (Fig. 2f). And based on the fact that the EHC process is isothermal in nature and through the increased profitability of hydrogen produced from EHCs (current hydrogen prices are around 11€ kg^{-1}) due to the price reduction in membrane-electrode-assemblies (MEA) [75], EHCs are expected to replace conventional mechanical compressors. Like PEMFCs, EHCs also possess other attractive advantages, including the potential for higher efficiency, lower or zero emissions, increased simplicity and reduced costs. As another significant advantage, the use of EHCs can allow for the extraction of hydrogen from gaseous mixtures in which although current global hydrogen consumption is estimated at 50 Mt y^{-1}, only ~4% is generated from electrolysis with the majority being produced from fossil fuels (~96%) along with small amounts from other sources such as medical and aerospace applications [76]. Recently, EHCs have also been applied to purify hydrogen similar to traditional pressure swing adsorption (PSA) and dense metal membrane techniques [77] in which Nordio et al. [78] compared EHC systems with PSA systems and reported that EHCs were more worthwhile in small-scale operations with elevated outlet hydrogen pressures. Moreover, EHCs have also been applied to coordinate MHCs in the effective reduction in operating costs [79–81].

Investigations into EHCs from different research institutes and companies have also revealed potential for future practical application. For example, ANALYTIC POWER conducted a two-stage approach to study EHCs as supported by the US DOE in 2005 due to the positive shifting in national policies on EHCs, and Fuel Cell Energy together with Sustainable Innovations were able to achieve a hydrogen pressure of 88.25 MPa in a single-stage mode and 41.37 MPa in a two-stage mode along with hydrogen recovery efficiency of over 98% by using EHCs. Other companies such as Proton Energy, Nuvera and H2Pump have also demonstrated hydrogen purification together with compressions up to 1.03 MPa by using EHCs along with pressures of 2.28 MPa (differential) by using polybenzimidazoles (PBI) as a membrane in 2012. In addition, Giner Inc. developed an EHC that can provide pressures of 87.5 MPa in a single-stage mode with a voltage of 0.159 V (each cell) and an inlet pressure of 10 MPa and also reported that maximum pressures up to 140 MPa can be achieved [82]. Grigoriev et al. [83] also developed an EHC that allowed for the compression of lower pressure into high-output pressure up to 13 MPa with

a flow rate of 0.01 N m^{-3}. Moreover, an EHC developed by HyET Hydrogen in the DON QUICHOTE project and the PHAEDRUS project achieved a compression up to 100 MPa [84] and in Japan, an EHC with an active surface area of 10 cm^2 was designed that demonstrated high pressures above 70 MPa under 1.2 A cm^{-2} through burst testing [85].

By comparing commonly used hydrogen compressors mentioned above, the advantages and disadvantages of different compressors are summarized in Table 1. Overall, EHCs are prominent technology for hydrogen compression based on their advantages.

3 Electrochemical Hydrogen Compressor

3.1 Principle of EHCs

For EHCs using PEMs, low-pressure hydrogen is usually converted into high-pressure hydrogen through direct current. Here compression can be divided into three steps as driven by an imposed cell voltage similar to the cathodic reaction of water splitting involving the anodic oxidation of molecular hydrogen to form protons, the migration of protons through the PEM and the cathodic reduction in protons to molecular hydrogen. As for electrons, they are transferred through an external circuit to cathode CLs to allow for the simultaneous mass transport and purification of hydrogen. Overall, the EHC process involves low-pressure hydrogen (P_a) being fed into the anode side in which hydrogen oxidation reactions (HORs) occur to split hydrogen into protons and electrons whereas hydrogen evolution reactions (HERs) occur at the cathode side to reform hydrogen. The corresponding electrochemical reactions are as follows:

$$\text{Anode: } H_2(P_a) \rightarrow 2H^+ + 2e^- \tag{3}$$

$$\text{Cathode: } 2H^+ + 2e^- \rightarrow H_2(P_c) \tag{4}$$

$$\text{Overall: } H_2(P_a) \rightarrow H_2(P_c) \tag{5}$$

in which P_c and P_a are the hydrogen pressures at the high-pressure cathode side and the low-pressure anode side, respectively.

The Volmer–Heyrocsky–Tafel mechanism can also be used to describe hydrogen electrode reactions [86] in which adsorbed hydrogen (H_{ad}) as a reaction intermediate species in hydrogen electrode reactions can be expressed by using three elementary reactions including the Volmer reaction, the Heyrovsky reaction and the Tafel reaction and the overall reaction can occur through either the Volmer–Heyrovsky route or the Volmer–Tafel route. All of these reaction routes can be represented as follows:

$$\text{Volmer: } H_{ad} \underset{v_{-V}}{\overset{v_{+V}}{\longleftrightarrow}} H^+ + e^- \tag{6}$$

$$\text{Heyrovsky}: H_2 \underset{v_{-H}}{\overset{v_{+H}}{\longleftrightarrow}} H_{ad} + H^+ + e^- \tag{7}$$

$$\text{Tafel: } H_2 \underset{v_{-T}}{\overset{v_{+T}}{\longleftrightarrow}} H_{ad} + H_{ad} \tag{8}$$

As for detailed mechanisms, they can be analyzed by using electrochemical impedance spectroscopy (EIS) with the spectra of the cathode displaying charge transfer rate-limiting features whereas the spectra of the anode exhibiting mass transfer rate-limiting features. Cathodic HER is dominated by the Volmer–Heyrovsky route and anodic HOR is dominated by the Volmer–Tafel route in which Chen and Kucernak [87] in their study proved that HOR follows the Volmer–Tafel reaction by using conventional ex situ characterization methods. Due to the slow reaction rate imposed by the Volmer–Heyrovsky route; however, cathodic HER requires high non-ohmic overpotentials. Despite this, HER kinetics can also increase by increasing cathode pressures, suggesting that the increased coverage of adsorbed hydrogen on catalyst surfaces can result in the reduction in non-ohmic overpotential for HER.

In EHCs, protons flow through a PEM and electrons flow through an external circuit to a cathode to eventually recombine into hydrogen molecules, thus resulting in the conversion of electrical energy into compression energy. Here, the reaction rate of hydrogen through PEMs can be calculated by using Faraday's law:

$$J_{H_2,\text{Theoretical}} = \frac{dn}{dt} = \frac{I}{2F} \tag{9}$$

in which n is the inlet hydrogen flow in mol, F is Faraday's constant (9.648×10^4 C mol^{-1}) and I is the current in A. In addition, the potentials of anodes and cathodes can be defined by using the Nernst equation as shown in Eqs. (10) and (11) and the relationship between the ratio of outlet gas and external circuit voltage can be calculated using Eq. (12):

$$V_a = E_0 - \frac{RT}{2F} \ln\left(\frac{P_a}{P_0}\right) \tag{10}$$

$$V_c = E_0 - \frac{RT}{2F} \ln\left(\frac{P_c}{P_0}\right) \tag{11}$$

$$V_{\text{Nernst}} = \frac{RT}{2F} \ln\frac{P_c}{P_a} \tag{12}$$

in which E_0 is the cell potential at standard conditions (considered 0 in the case of electrochemical compression), R is the universal gas content (8.3144 J mol^{-1} K^{-1}) and T

Table 1 Different characteristics of common hydrogen compressors

Category	Reciprocating piston compressors	Diaphragm compressors	Ionic liquid compressors	Cryogenic compressors	Adsorption compressors	Metal hydride compressors	Electrochemical hydrogen compressors
Outlet pressure (MPa)	100	51.7	100	35–90	35	70	70–100
Typical capacity ($N\ m^3\ h^{-1}$)	300	50–280	376–753	> 1000	72.6	2	0.93–1
Advantages	Mature technology Flexibility in size and capacity	Mature technology High throughput Low cooling requirements Ideal for pure gases	Fewer moving parts (compared to the first two) Long lifetimes High efficiency Low-energy consumption	High hydrogen density High volumetric efficiency High gravimetric and volumetric capacities	No moving parts Simple design No noise Thermal energy driven Low cost	No moving parts Simple design No noise Thermal energy driven	No moving parts Simple design No noise Low energy cost High efficiency Hydrogen purifier Modular Rapid compression
Disadvantages	Moving parts Contamination and danger due to lubrication oils (if used) System complexity Vibration Noise High heat loss Low efficiency High-cost	Moving parts Low durability (diaphragm failure) Low flow rates System complexity	Possibility of leaking System complexity	Low temperatures Low durability High vacuum quality required High gravimetric and volumetric capacities	Limited heat transfer Additional cooling system required High vacuum quality required Low reaction temperature	Slow compression time Limited heat transfer Low efficiency Low durability	Hydrogen back-diffusion Designed water management High-strength accessory design required

represents the temperature of hydrogen at the anode side. And although the theoretical voltage for hydrogen compression is only related to pressure difference and operating temperature based on the Nernst equation, the voltage of practical EHCs can be affected by several factors, including catalyst activity and PEM ion conductivity in which for voltage loss caused by catalysts and membranes, they can be classified into three causes, including activation overpotential-related to electrocatalysts, ohmic overpotential related to proton transport through PEMs and mass-transfer overpotential. Rochilz et al. [75] were also able to develop a zero-dimension and stable EHC model to calculate overall voltages by considering ohmic overpotential and activation overpotential and reported that different overpotentials can be separated based on anodes and cathodes. As for current density j applied to EHC cells, Eq. (13) can be used to express cell voltage V_{cell}:

$$V_{cell}(j) = V_{Nernst} + V_{AnodeOhmic}(j) + V_{AnodeNonohmic}(j) + V_{CathodeOhmic}(j) + V_{CathodeNonohmic}(j) \quad (13)$$

Furthermore, the efficiency of EHCs can be classified into voltage efficiency and current efficiency in which voltage efficiency is defined by dividing theoretical voltage by cell voltage as expressed by Eq. (14), whereas current efficiency is defined by dividing the real amount of compressed hydrogen by the theoretical value as expressed by Eq. (15). Moreover, the overall efficiency of EHCs can be determined by both voltage and current efficiency as expressed by Eq. (16).

$$\eta_V = \frac{V_{Nernst}}{V_{cell}} \quad (14)$$

$$\eta_I = \frac{J_{H_2,Real}}{J_{H_2,Theoretical}} \quad (15)$$

$$\eta_{EHC} = \eta_I \times \eta_V \quad (16)$$

3.2 Operating Temperature of EHCs

The operating temperature of EHCs is highly dependent on the performance of membranes and in general, EHCs can be divided into low-temperature EHCs with low-temperature PEMs as membranes (e.g., Nafion), high-temperature EHCs with high-temperature PEMs as membranes (e.g., acid-doped PBI) and solid oxide EHCs with perovskite-type oxides as membranes [e.g., $Ba(Zr_{0.30}Ce_{0.54}Y_{0.15}Cu_{0.01})O_{3-\delta}$].

3.2.1 Low-Temperature EHCs

In terms of low-temperature EHCs, because the ion conductivity of perfluorosulfonic acid (PFSA) is highly dependent on water uptake, EHCs employing PFSAs such as Nafion as membranes can only operate at temperatures lower than 100 °C with operating temperatures normally ranging from 50 to 90 °C if considering catalyst activity. In recent years however, sulfonated hydrocarbon membranes such as SPEEK have also been employed as membranes due to low costs and high conductivities [88, 89]. And in general, single-stage low-temperature EHCs are more suitable for small-scale compressions.

3.2.2 High-Temperature EHCs

As for high-temperature EHCs, phosphoric acid-doped polymers (e.g., the PBI/H_3PO_4 complex) are usually used to conduct protons. Various acids have also been studied for doping with PBI membranes, including HCl, HNO_3, H_2SO_4 and $HClO_4$, to allow for the conduction of protons with doped acids instead of hydrated protons and result in EHCs with these acid-doped polymers being considered as promising candidates for high-temperature EHCs at temperatures above 100 °C. These high-temperature EHCs are also promising due to associated cost reductions and reliability improvements through the elimination of issues in low-temperature EHCs in terms of water management, heat rejection, catalyst tolerance and reaction kinetics [90]. Furthermore, researchers have reported that the dipping of PBI in aqueous phosphoric acid to form an acid-base complex can result in enhanced proton conductivity, lowered gas permeability and a nearly zero water drag coefficient at high temperatures even in an anhydrous state. Moreover, the elevated operating temperatures of high-temperature EHCs can provide excellent thermal stability, a nearly zero water drag coefficient and improved impurity tolerance (especially carbon monoxide) for Pt catalysts as compared with low-temperature EHCs and the notorious flooding issue in the electrodes of low-temperature EHCs can be prevented due to the gaseous form of water at high temperatures.

3.2.3 Solid Oxide EHCs

Perovskite-type oxides such as $Ba(Zr_{0.30}Ce_{0.54}Y_{0.15}Cu_{0.01})O_{3-\delta}$ can conduct protons at 600–900 °C. Based on this, solid oxide EHCs that are similar to solid oxide fuel cells and solid oxide water electrolysis systems have been proposed in recent years [91, 92]. Here, protons in solid oxide EHCs move through a lattice through a hopping process that is generated by water hydration reactions [93] and as compared with other fuel cell technologies, the main benefit of solid oxide EHCs is the existence of a solid electrolyte

that can avoid the need for corrosive environments. Another great advantage of solid oxide EHCs is fuel flexibility in which a variety of hydrocarbon fuels can be used. Moreover, the production of hydrocarbon fuels such as ammonia can occur during hydrogen compression, thus allowing for the reduction of total costs for hydrogen compression [94, 95]. Furthermore, solid oxide EHCs are also suitable as large stationary compressors.

4 Components of Electrochemical Hydrogen Compressors

4.1 Membranes

PEMs are critical components in EHCs and need to possess high proton conductivities, good mechanical properties and low gas crossover rates [84] in which PEM proton conductivities can affect the efficiency of EHCs and good mechanical strength is needed to ensure the integrity of membranes under high-pressure. Here, HyET hydrogen and NREL have committed great efforts to the defect characterization of EHC membranes and the design of databases [96] in which to develop durable PEMs, the exploration of degradation mechanisms, especially the effects of mechanical stress in EHCs, is vital.

As for hydrogen back-diffusion, it occurs due to the existence of partial pressure differences between anodes and cathodes and is affected by many factors including the water content, temperature, membrane thickness and pressure [97]. In terms of the water content, the proton conductivity of PFSA membranes is strongly dependent on the water content and temperature in which water is needed to guarantee good proton conductivity in PEM hydrophilic phases because protons can move into hydrated sections through the dissociation of sulfonic acid bonds. Here, a low water content can cause PEM dehydration due to increasing operating temperatures and result in decreased proton conductivity whereas well-hydrated membranes can better accommodate increasing temperatures to enhance proton conductivity in which low conductivities can limit the access of protons to catalyst surfaces, reduce the number of reactive active sites in CLs and increase activation polarization [98]. And in cases of a very low water content, severe drying can occur that will lead to irreversible degradation (e.g., delamination, pinholes) [99] to result in significantly increased ohmic resistances. Alternatively, excess water can block catalyst sites and cause water flooding to result in poor performance. The water content in EHCs can also affect the swelling ratio of PEMs in which as the water content increases, the swelling ratio of PEMs also increases and can cause increased hydrogen back-diffusion [100].

System temperatures have a remarkable effect on transportation, including water diffusion, permeability and proton conductivity, and the influence of temperature on hydrogen crossover can be determined based on the hydrogen permeability coefficient that is closely related to temperature and can be expressed as the Arrhenius form [101]:

$$\ln \Psi_{H_2}^{PEM} = \ln \Psi_{H_2}^{o} + \left(-\frac{E_{H_2}^{PEM}}{R} \right) \frac{1}{T} \tag{17}$$

in which $\Psi_{H_2}^{PEM}$ represents the hydrogen permeability coefficient, $\Psi_{H_2}^{o}$ is the maximum permeability coefficient (e.g., at infinite temperature), $E_{H_2}^{PEM}$ is the activation energy for hydrogen crossover, R is the gas constant and T is the temperature in Kelvin. Based on this equation, it can be seen that hydrogen permeability coefficients increase with increasing temperature. Here, researchers reported that temperature decreases from 80 to 21 °C can lead to hydrogen gas permeability ratio decreases of 3 and 5 orders of magnitude under cathode pressures of 70 and 30 MPa, respectively [102]. Truc et al. [103] also proposed a numerical model for hydrogen crossover and the dependence of permeability on the membrane water content and temperature and reported that the reduction in EHC operating temperature can slow down hydrogen back-diffusion, particularly in the case of high-pressure differentials and thin or commercial membrane materials with greater porosity. As a result, optimum membrane operating temperatures for EHC applications can only be achieved through a compromise between high proton conductivity and low hydrogen back-diffusion to minimize overall energy requirements for compression [104].

As for the impact of pressure on hydrogen back-diffusion, there is a universal agreement that hydrogen back-diffusion rates increase with increasing outlet pressures at any temperatures and RH (the water content of membrane) and that increased hydrogen back-diffusion rates will lead to performance degradation and efficiency reduction [105]. Here, gas pressure applied on each side of EHC membranes is balanced with the solubility coefficient (H_i) (mol m^{-3} Pa^{-1}) of the facing side to form a concentration gradient in the corresponding PEM, which can cause gas permeation from one side of the membrane to the other in which the gas permeation rate (N_i) of species i through a membrane can be expressed as:

$$N_i = D_i \frac{H_i^h p_i^h - H_i^l p_i^l}{\delta} \tag{18}$$

In addition, the definition of k_i, which is the gas molar permeability coefficient (mol m^{-1} s^{-1} Pa^{-1}), can be expressed as:

$$k_i = D_i H_i \tag{19}$$

in which D_i is the effective diffusion coefficient in $cm^2\ s^{-1}$, p_i is the partial pressure of gas (Pa), and δ is the thickness of the membrane.

And as a key parameter in the above equations, the thickness of membranes can significantly affect performance in which for thick PEMs, water distribution becomes uneven, thus leading to uneven current distributions and current hotspots as well as membrane swelling [106]. The thickness of PEMs can also cause ohmic loss, which can further lead to power loss. Therefore, although thick PEMs are usually used in EHCs due to their high mechanical strength under pressure, optimal PEMs in EHCs need to be simultaneously thin and robust.

Overall, all of the above controllable factors are crucial in the determination of hydrogen back-diffusion and the performance of EHCs. And in order to focus on electrochemical purification, EHC cells should operate with a zero total pressure gradient across the PEM. As for one-step EHCs, total pressure gradients can vary significantly between different experiments and because several cells are usually included in a single stack, even if overall compression ratios are specified, it is difficult to know the pressure difference on either side of PEMs for individual cells within the stack. Nevertheless, 5 MPa is commonly accepted as the large pressure gradient for low-temperature commercial PEMs whereas in laboratory settings, higher-pressure gradients can be achieved with higher compressions (a positive effect) due to the use of reinforced or high-temperature membranes. However, such large gradients can also cause increased gas permeation and back-diffusion (a negative effect). In summary, the proton conductivity, the mechanical property and the back-diffusion rate are three critical properties for PEMs in EHCs.

As for the membrane design of EHCs, it is based on predesigned operating conditions (specifications), including inlet and outlet pressure, lifetimes, duty cycles, operating expense and capital expenditure, in which the total active area of membranes needs to be first defined followed by the consideration of operating current density, the compression ratio and optimal temperature for selected materials [84]. And based on a 3D graph of the properties of a proprietary low-temperature membrane visualizing energy requirement as a function of current density and the compression ratio (Fig. 3a), a positive correlation between energy requirement and current density exists based on Ohm's law in which all energy is converted into heat at zero compression ratio (i.e., $P_{in} = P_{out} = 10$ bar). At elevated cathode pressures, energy requirements also show a vertical tangent with low-current densities due to the compensation of the Faradaic compression rate by back-diffusion. And because these correlations are also appropriate for membrane thickness and materials, specific energy requirements can be optimized by adjusting membrane thickness or materials accordingly. Alternatively, high-temperature membranes suffer less hydrogen back-diffusion as compared with low-temperature membranes (Fig. 3b). In conclusion, the operation of lower current densities requires lower energy and corresponding membranes are more suitable for higher compression ratios. Based on these characteristics, several types of polymer membranes have been used in EHCs, including perfluorosulfonic acids (PFSAs) (e.g., Nafion), ion-solvating polymers (ISPs) (e.g., polybenzimidazole), hydrocarbon polymers (e.g., sulfonated-polyether-ether-ketone) and proton-conducting oxides.

4.1.1 Perfluorosulfonic Acids

Currently, PFSAs combined with hydrophobic backbones and hydrophilic side chains are the most widely used membranes in EHCs due to good chemical stability, high proton conductivities and excellent physical properties [107, 108]. Catalano et al. [109] were also able to formulate a theoretical framework with non-equilibrium thermodynamics to describe electro-kinetic effects in gas–liquid two-phased membranes based on Nafion 117. Despite this, the large-scale application of PFSA polymers in EHCs is limited by extensive hydrogen back-diffusion, management of the water content, low mechanical strength and high costs and up to now, the reduction of back-diffusion rates under high-pressure differences in EHCs remains difficult [104, 110]. Here, two main methods can be used to suppress hydrogen back-diffusion involving the use of thick membranes and the doping of materials to decrease the water content. For example, Analytic Power Corp. used Nafion 117 rather than Nafion 112 as a membrane in their EHC [111] because Nafion 112 with a thinner membrane led to larger hydrogen back-diffusion during high-pressure power consumption per unit hydrogen as compared with Nafion 117 due to higher resistivity. Stobel et al. [112] also studied the effects of PEM thickness on back-diffusion and found that PEM thickness was a crucial design parameter to balance back-diffusion and proton resistance and that increasing temperatures can lead to higher hydrogen back-diffusion rates. Alternatively, Sdanghi et al. [113] proposed that membrane thickness affected the water content, which in turn can influence the overall performance of EHCs. Hence, the influence of membrane thickness on back-diffusion needs to be comprehensively investigated. In a further study, Grigoriev et al. [83] found that zirconyl phosphate (ZP) particles can replace un-bonded water molecules in PEMs and this replacement is beneficial for the modification of membrane hydration levels to allow for the reduction in hydrogen back-diffusion (Fig. 3c). Despite this, these researchers also found that internal resistances increased as a result of the modification, which led to lowered compression efficiency in the corresponding EHC.

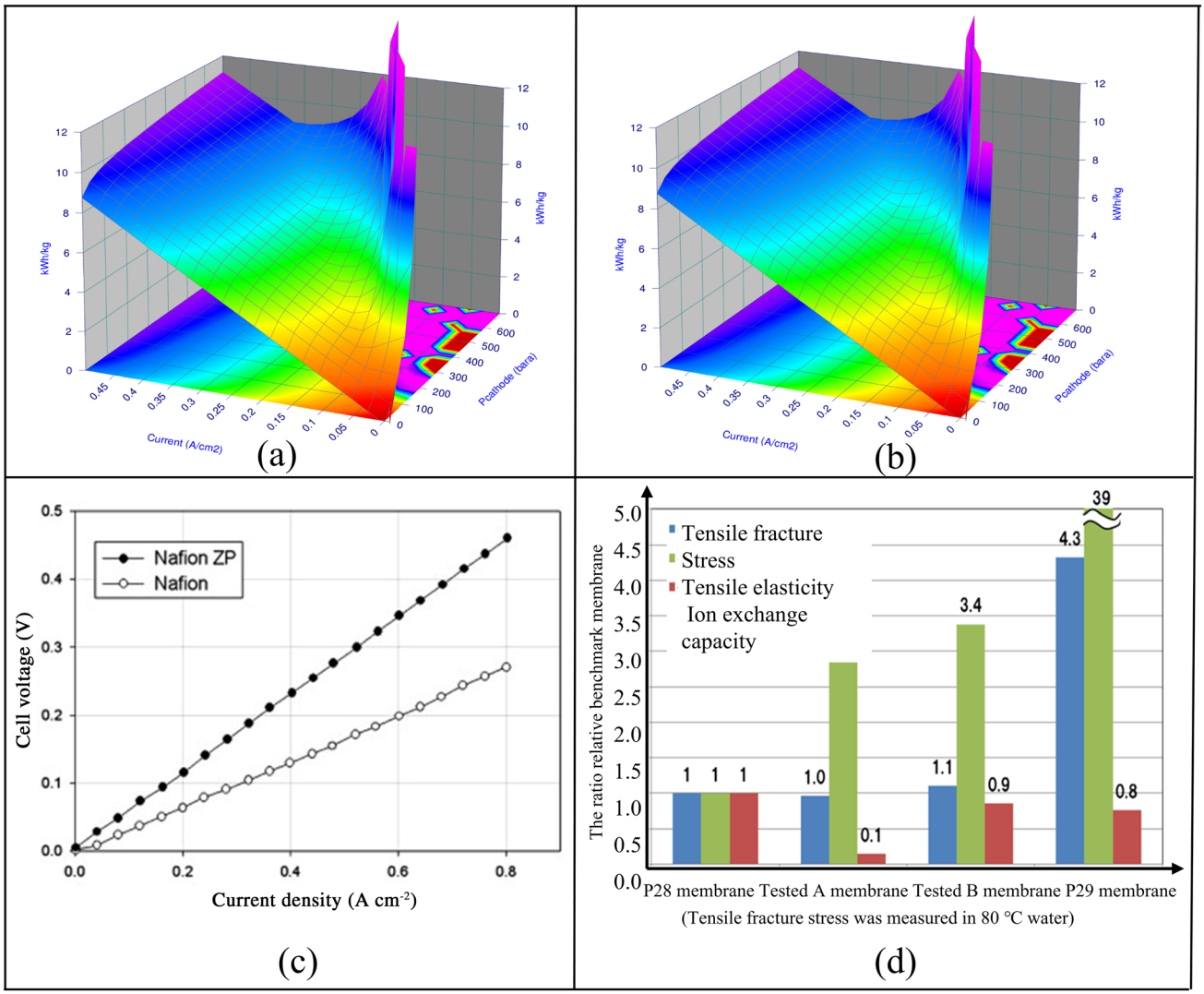

Fig. 3 (**a**) Typical 3D graph showing calculated hydrogen compression energy as a function of current density and cathode pressure based on low-temperature membranes. Reprinted with permission from Ref. [84]; copyright of CRC Press. (**b**) Typical 3D graph showing calculated hydrogen compression energy as a function of current density and cathode pressure based on high-temperature membranes Reprinted with permission from Ref. [84]; copyright of CRC Press. (**c**) Comparison of *I–V* curves obtained on the compression cell (0.8 mg cm^{-2} of Pt for both the anode and the cathode) with unmodified (the empty circle) and ZP-modified (the filled circle) SPE membranes. Reprinted with permission from Ref. [83]; copyright 2010 Elsevier B.V. (**d**) Characteristics of a membrane made by NEDO. Reprinted with permission from Ref. [85]. Sources from Japan, The New Energy and Industrial Technology Development Organization

The addition of other inorganic compounds has also been explored to increase water uptake within polymer matrices, including SiO_2 [114], TiO_2 [115] and $Al_2Si_2O_5(OH)_4{\cdot}nH_2O$ [116]. Furthermore, researchers have reported that the use of low water content hydrogen as a feedstock can reduce the power input requirements for water evaporation and increase overall hydrogen compression efficiency [83]. Giner ELX Inc. also developed a modified PFSA membrane with a back-diffusion loss of 27% at 35 MPa in which as compared with an unmodified PFSA membrane, the back-diffusion rate in the modified membrane was reduced by more than 50% whereas the energy consumption of an EHC using the modified PFSA membrane was 2.0 kWh kg^{-1} at 0.5 A cm^{-2} under 35 MPa [82]. Moreover, McDonald et al. [117] reported that the mixing of a quaternary monomer can affect the polymerization of the monomer to exhibit increased strength and reduce permeability to water and gas as well as proton conductivity and acidity in which by modifying certain interior regions of the membrane, the membrane was divided into multiple sealed segments. Similarly, HyET hydrogen also mentioned membranes with high differential pressure characteristics in a patent filed in 2010 [118].

In general, the high-pressure conditions of EHCs can not only cause serious hydrogen back-diffusion issues but also

accelerate membrane degradation due to high mechanical stress to accelerate the chemical degradation of PFSA membranes in which resulting defects can be observed through optical imaging to identify in situ defect formation [96] and from corresponding EHC performances. In addition, the release rate of fluoride in Nafion 117 at various applied pressures also possessed a positive correlation with compression pressure [119] in which the deformation accumulation of membranes can lead to polymer decomposition and lowered activation energy in decomposition reactions [119, 120]. Based on this, Greenway Inc. was able to develop a Nafion 117 membrane that can endure temperatures of 130–150 °C and up to 10 MPa for both EHCs and MHCs [121]. And by considering the fact that the boiling point of water is 150 °C at 0.5 MPa, PFSA can potentially operate well at temperatures beyond 100 °C with stable proton conductivity [122].

More attention also needs to be paid to the separation of hydrogen from various gas mixtures in PFSA-based EHCs [83, 123]. Here, Gardner et al. [124] demonstrated that the issue of CO contamination can be resolved to improve hydrogen separation efficiency by periodically pulsing voltage to oxidize absorbed CO. Casati et al. [125] also found that hydrogen recovery increased and performance coefficients (defined as the ratio of hydrogen produced to hydrogen consumed) decreased with differences in applied potential. Based on these results, optimal energy efficiency for separation should be provided and its functional dependence on process parameters in separating H_2 from H_2/N_2 mixtures should be identified. Here, Abdulla et al. [108] developed single-stage and multi-stage gas recovery prediction models to study the separation of mixed gases, including CO_2, water vapor and hydrogen, and found that the multi-stage recovery model can achieve 90% energy efficiency and 98% hydrogen recovery. Using these models, these researchers were also able to confirm that membrane resistances and mass transfer coefficients of GDLs at the anode were two critical parameters of EHCs.

4.1.2 Hydrocarbon Membranes

Despite widespread usage, Nafion possesses inherent drawbacks such as high costs, limited operation temperatures and gas crossover [126]. Alternatively, polyaromatic hydrocarbon membranes have emerged as popular candidates for EHCs, especially PEEK, due to low permeabilities (owing to narrower channels), high thermal and mechanical stability and low prices. In general, hydrocarbon membranes are synthesized through a simple sulfonation reaction involving the grafting of a sulfonic acid group into a polyether-ether-ketone chain in which the resulting proton conductivity depends on the degree of sulfonation (DS). However, these hydrocarbon membranes usually possess poor proton conductivity due to the poor compatibility of imidazole ionic liquid-based composite membranes with Pt catalysts. In addition, continuous operations using these membranes often result in losses of ionic liquid. To resolve these issues, great efforts have been devoted to the investigation of improvement strategies for the various properties of hydrocarbon membranes (e.g., mechanical property, dimensional stability, proton conductivity) through methods including blending with other polymers [127], cross-linking [128] and the addition of inorganic fillers [129].

The physicochemical characterizations of these modified membranes and corresponding EHC performances have also been widely investigated. For example, Rico-Zavala et al. [130] studied membranes based on SPEEK prepared through the impregnation of Halloysite nanotubes with phosphotungstic acid (PWA) and Halloysite nanotubes (HNTs) and found that the incorporation of fillers can reduce water uptake and swelling (area and volume) through the effective modification of SPEEK membranes in which as compared with benchmark [S70] membranes (3.873×10^{-8} mol bar^{-1} s^{-1} cm^{-2}), the modified {[S70/HNT_{15}] and [S70/$(PWA/HNT_{30})_{15}$]} membranes showed lower back-diffusion rates of 7.296×10^{-10} and 9.103×10^{-10} mol bar^{-1} s^{-1} cm^{-2}, respectively. These researchers also reported that proton conductivities were increased by 42% and 88% for membranes impregnated with HNTs and $(PWA/HNT_{30})_{15}$, respectively, and concluded that the presence of HNTs can improve the mechanical strength of composite membranes whereas the presence of PWA mainly gave rise to high proton conductivity, thus demonstrating that modified nanocomposite membranes can present low-energy consumption at high pressure [88, 130].

Moreover, a "P29 series" hydrocarbon membrane developed by NEDO in Japan showed higher tensile stresses, elastic rates and better performances in EHCs than membranes developed in 2018 by Toray Industries (Fig. 3d) [85] and Giner ELX Inc. developed multiple hydrocarbon membranes such as BPSH and biphenyl series membranes (BP-ArF_4, BP-ArSA, BP-SA) for EHCs to report that their biphenyl series membranes can display higher proton conductivities at lower ion exchange capacities with less swelling in water [131]. In addition, Giner ELX Inc. also reported that their BP-ArF_4 membrane demonstrated a much reduced back-diffusion loss of 7% at 35 MPa as compared with a BPSH membrane (20%) and that an EHC using BP-ArF4 and BPSH membranes exhibited the lowest cell voltage of 0.100 V $cell^{-1}$ at a current operating density of 1000 mA cm^{-2} [132].

Many other types of membranes have also been explored of use in the specific work environment of EHCs. For example, to overcome the problem of water management, Yang et al. [133] developed a water-free PEM that can operate in temperatures ranging from 120 to 180 °C in which at a low compression ratio of 1.5, a voltage of 0.073 V at 2 mA cm^{-2} was obtained as well as a proton transport number in the

range of 0.17–0.20. Sustainable Innovations also conducted a cutting-edge study of phosphoric acid-doped aromatic polyether (PA-APE) for EHCs with promising results [134] and Wu et al. [89] synthesized a semi-interpenetrating network (sIPN) containing a SPEEK membrane and a cross-linked polystyrene sulfonic acid. In this study, these researchers reported that the use of their SPEEK/CrPSSA membrane resulted in the rapid increase in current to the limited current, which indicated high mass-transfer resistance and that the energy efficiency of the corresponding hydrogen compressor was ~ 30%.

The study of durability has also been conducted based on realistic drive cycles. For example, Lipp et al. [135] completed a 10000 h durability test compressing hydrogen from 0.2 to 20.4 MPa and set a US compression record of 81.6 MPa with energy consumption of ~ 20 kWh kg^{-1} in which a possible correlation existed between observed degradation behaviors and local mechanical stress experienced in EHCs.

4.1.3 Protonic Ceramic Membranes

Proton-conducting oxide membranes for EHCs can typically operate at high temperatures of 800–900 °C and therefore have gained attention in EHC processes focused on the purging of impurities in hydrogen. In addition, these materials can potentially be used as electrolytes for the separation of hydrogen from reformed natural gas despite low conductivities. For example, Catalano et al. [109] investigated Ba$(Zr_{0.30}Ce_{0.54}Y_{0.15}Cu_{0.01})O_{3-\delta}$ as a protonic ceramic membrane in which Y and Zr were added as dopants to improve chemical stability against steam and CO_2 whereas Cu was added as a dopant to enhance sintering ability and reported that the corresponding EHC demonstrated excellent performances at a current density of 2 A cm^{-2} at 973 K. Sakai et al. [91] also found that $La_{0.9}Ba_{0.1}YbO_{3-\delta}$ (LBYb-91) possessed high chemical stability against CO_2 contamination based on post-mortem XRD and TGA analysis and reported that the total cell voltage of an LBYb-91 EHC can reach ~ 0.7 V at 800 °C with an applied current density of 40 mA cm^{-2}. Despite these performances however, harsh working temperatures remain a serious issue that limits large-scale research and promotion as high-temperature EHCs. Regardless, the study of relationships between physical properties and nanostructures in protonic ceramic membranes such as proton mobility and gas permeability for EHC applications remains popular in the development of high-temperature EHCs. However, membranes designed for operation with pressure differences across membranes that are significantly affected by spacing, domain segregation, crystallization and the presence of water and electric fields were not further investigated. Overall, the meticulous design of protonic ceramic membranes with superior membrane support can significantly increase compression capability in which the fabrication of multilayered dense thin membranes with porous and robust support layers to reduce thickness is a viable strategy. In addition, the use of robust membrane supports can improve corresponding mechanical and thermal stability in membranes.

However, due to the lack of data concerning the membrane creep and long-term performance in the literature, the summarization of correlations between mechanical property and operational property in protonic ceramic membranes is difficult. As a result, significant research needs to be conducted on EHC protonic ceramic membranes in the future. In addition, due to intricate interactions among microscopic structures, membrane composition, reorganizations upon swelling and effective material properties (strain, stress, modulus) along with statistical fluctuations in pore ensembles, the comprehensive understanding of protonic ceramic membrane characteristics in EHCs also remains difficult.

4.1.4 Ion-Solvating Polymers

Due to PFSAs exhibiting large hydrogen back-diffusion rates as well as the release of corrosive gas after degradation, alternative membranes have been investigated in the last decade. Here, PBI is a high-temperature membrane with an operating temperature between 160 and 220 °C and therefore can demonstrate high-temperature operational capabilities. And because PBI membranes are generally doped with phosphoric acid to form an ion-solvating polymer (ISP), advantageous properties can be attained, including low back-diffusion [136], zero electron osmotic draw [137], high tolerance against impurities and facile water management in which the doped acid in PBI membranes is used to conduct protons. Because of this, the conductivity of corresponding membranes is directly dependent on the level of acid doping. And as result of this unique merit, acid-doped PBI membranes can operate at high temperatures (160–220 °C). However, because doped acids interact with PBI backbones through weak Van Der Waals forces, the progressive release of doped acids during EHC operation can also occur, which will cause gradual increases in internal resistance and significantly reduce the compression efficiency of EHCs.

More significantly, the higher operating temperatures achieved in the use of PBI membranes can enhance the tolerance of impurities such as CO and CO_2 [138–140] to reduce the inhibition of electrochemical activity for both anodic and cathodic reactions. For example, although industrial hydrogen is inevitably mixed with impurity gases, including CO or CO_2, the concentration of CO can be successfully reduced by more than 150 folds from 1906 to 12 ppm and the concentration of CO_2 can be successfully reduced by 32 folds and 62 folds from 11.9% to 0.37% and from 11.9% to 0.19%, at 0.4 and 0.8 A cm^{-2}, respectively, through the use

of corresponding EHCs [139]. Moreover, Thomassen et al. [141] found that the performance of a PBI membrane-based EHC supplied with a reformate mix containing 100 ppm CO was nearly identical to a cell running on 40% hydrogen in nitrogen, demonstrating that the CO content did not affect catalyst activity at low concentrations and that reformate species only had a diluting effect. These researchers also reported, however, that cells fed with reformate gas containing 1.36% CO can experience larger increases in cell voltage at high current densities despite increasing hydrogen concentrations, indicating that enhanced CO concentration in inlet gas can decrease EHC performance. Moreover, these researchers also found that the PBI membrane displayed excellent abilities to purify H_2–CO_2 mixtures in which a 21% CO_2 content in a H_2–CO_2 mixture was reduced by over 98% at different current densities (Table 2). Strikingly, Robeson et al. also reported that both PFSA and PBI membranes can show enhanced performances in the separation of mixed gases at 230 °C, which is far beyond upper operating temperature limits. Sustainable innovations LLC also developed a phosphoric acid-doped polybibenzimidazole (PA-PBI) membrane for in-depth testing in which the resulting PA-PBI membrane was subjected to various testing conditions including the variable inlet CO_2 content, the inlet relative humidity and the reaction temperature with Nafion 117 as a benchmark (Fig. 4) [134]. Based on the results however, these researchers concluded that due to the release of acid during long-running operation, their PA-PBI membrane was not a good choice for EHCs. And aside from the acid leakage of membranes, the control of the polyphosphoric acid content is also critical in PBI membranes in which effective catalyst areas can sharply decline due to the adsorption of concentrated phosphoric acid [142]. Furthermore, Pingitore et al. [143] synthesized a poly(2,2′-(1,4-phenylene)5,5′-bibenzimidazole) meta/para-PBI random copolymer through a poly (phosphoric acid)

Table 2 Concentrations of CO_2 in the cathode outlet and relative reduction in CO_2 concentration in the separated hydrogen of a PBI membrane-based EHC [141]. Sources from the US Department of Energy

Current density (A cm^{-2})	Cathode outlet CO_2 concentration (%)	Reduction in CO_2 concentration (%)
0.5	0.4 ± 0.05	98
1.0	0.21 ± 0.09	99
1.5	0.11 ± 0.04	99.5

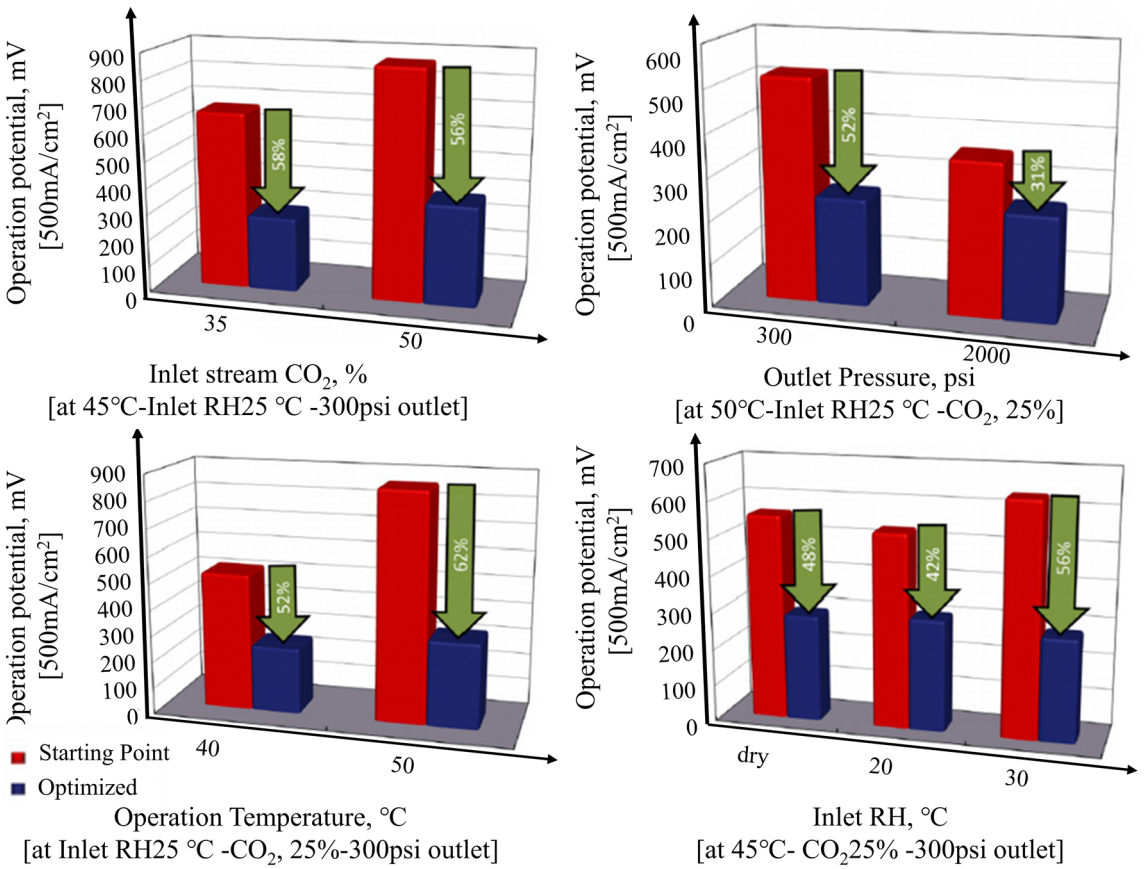

Fig. 4 Parametric testing of an EHC with flow field modifications. Reprinted with permission from Ref. [134]. Sources from the US Department of Energy

process in which the compressive creep compliance was less than 2×10^{-6} Pa^{-1} and reported that this membrane exhibited a high proton conductivity of 150 mS cm^{-1} at typical operating temperatures of 160–200 °C and an exceptionally low-voltage decay of 0.67 μV h^{-1} at 160 °C for more than 2 years.

Researchers have also reported that gases mixed with water vapor can accelerate the leakage of doped acid in PBI membranes. For example, Bueltea et al. [142] reported a cell voltage increase from 15 to 450 mV with a supply gas dew point decrease from 60 to 20 °C in 250 h in which the power requirement of the un-humidified supply gas was 30 times higher than that of the humidified gas. Power consumption has also been found to be highly sensitive to water vapor pressure in gas stream supplies, which also depends on the concentration of phosphoric acid-based PBI membranes. However, Yang et al. [144] found that the existence of water vapor in feed gas streams did not significantly affect the permeability of H_2 and CO_2 or the selectivity of H_2/CO_2 due to the super thermal stability of their ZIF-8/PBI nano-composite material in hot steam, especially in 30% and 60% ZIF-8 composites. Perry et al. [139] also achieved long-term durability for nearly 4000 h under non-humidified and humidified conditions using their PBI membrane and attributed the lower-power requirement of their humidified operation to lower losses in the CL. Moreover, Buelte et al. [142] reported that anode side gases of PBI-based EHCs still require humidification with water vapor pressures greater than 55 mmHg (a dew point of 40 °C) to allow for efficient operations.

In terms of application, H2Pump LLC in 2012 was able to develop a third-generation PBI-based EHC with an area of 50 cm^2 that operated for more than 1000 h at a differential pressure of 2.275 MPa whereas a single-cell operated for 4000 h at the same pressure [145]. Greenway Inc. also applied an MHC and an EHC as smart technologies in a new hybrid solid-state hydrogen compressor system in which four constitutive membranes [Nafion 212, PBI, an Advent membrane (a Pyridine-based aromatic polyether electrolyte) and a Fumatech membrane] were chosen as the membrane for the MEA of an EHC (Table 3) and found that although Nafion 212 in the EHC system possessed a slightly lower cell voltage than that of the PBI membrane, it did not provide any heat recovery opportunities for the MHC [131] (Fig. 5).

Overall, low operation temperatures can mitigate back-diffusion, particularly in situations (with back-diffusion of hydrogen gas) encountered with high-pressure differentials, thin thicknesses and high porosity in corresponding membranes. And in cases in which the hydrogen source is pure as a result of electrochemical water splitting, the mechanical properties of membranes are more important factors than the contamination of impurity gases in the use of high-temperature membranes. And based on overall design, the optimal balance of these characteristics is different for different applications. Furthermore, current membranes as reported by researchers have not been designed for operation under different pressures and therefore, membrane supports may be useful in the improvement of anti-compression ability. However, the absence of data on the creep and long-term properties of high-pressure membranes makes it difficult to establish accurate relationships between mechanical properties and membrane lifespans. As for the prevention of mechanical failure in ISP membranes, membrane clamping systems should be carefully designed to avoid uneven mechanical stress distribution and membrane reinforcements or modifications in polymer chemistry are also needed to reduce the creep characteristics of PFSA membranes. Here, membrane reinforcement can be achieved through the incorporation of inert, non-conducting reinforcement materials [58] and the combination of self-humidifying designs.

4.2 Electrocatalysts and Catalyst Layers

Catalysts play an essential role in EHCs to decrease the activation energy of reactions and promote the electrochemical kinetics of both HOR and HER. Therefore, the category, the dosage, the structural design and the durability of catalysts for EHCs need to be further studied. And because gases, electrons and protons all participate in the electrochemical reactions of EHCs on catalyst surfaces in which all species can access, it is necessary to improve the microstructure of CLs to obtain

Table 3 Membrane properties of an EHC system developed by Greenway Inc. Reprinted with permission from Ref. [121]. Sources from the US Department of Energy

Metric	Nafion®	PBI Film®	Advent®	Fumatech®
Operating T (°C)	60–150	120–180	120–200	160–180
Membrane thickness (μm)	N212 = 50 N211 = 25 N115 = 125	70	N/A	53
Membrane area (cm^2)	500	500	N/A	500
Range of current density (A cm^{-2})	1–4	1–4	1–4	1–4
Membrane conductivity (Ω cm^{-1})	0.5–0.11	0.1	0.08	0.1
Electrolyte	PFSA	PA	PA	PA
Water crossover (kg H_2O kg H_2^{-1} h^{-1})	28.5	Negligible	Negligible	Negligible

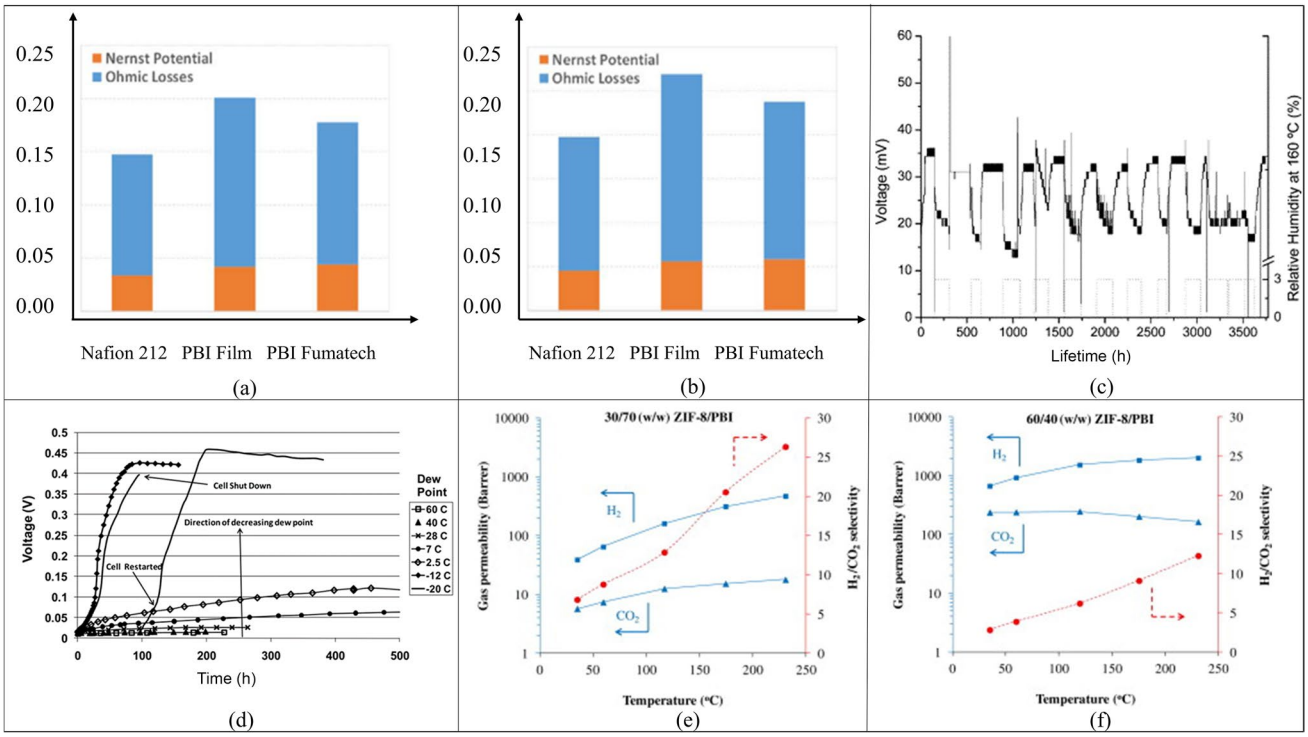

Fig. 5 (**a**) Technical performance comparisons between Nafion and PBI membrane systems. Reprinted with permission from Ref. [131]; Sources from the US Department of Energy. (**b**) Long-term operation of a hydrogen pump under alternating non-humidified and humidified conditions (0–3% RH) at 160 °C. Reprinted with permission from Ref. [139]; copyright 2007 Elsevier B.V. (**c**) Hydrogen pump cell voltage increases as the anode supply gas dew point decreases, operating conditions: 160 °C, 0.2 A cm^{-2} and with pure hydrogen anode supply gas. Reprinted with permission from Ref. [142]; copyright of The Electrochemical Society. (**d**) H_2/CO_2 mixed gas permeation results of a ZIF-8/PBI nano-composite membrane (solid lines—H_2 and CO_2 permeability; dotted lines—H_2/CO_2 selectivity) [144]; copyright 2013 Elsevier B.V

high efficiency 3D contact points and avoid the low utilization of Pt catalysts. The loading of precious metal Pt in CLs remains a costly issue that severely hinders the popularization of PEM-based devices in which in the initially proposed concept of an EHC by Sedlak et al. [146] in 1981, a Pt-based catalyst with a loading of 4 mg cm^{-2} was required. However, additional research has significantly lowered this loading to 0.2–0.8 mg cm^{-2} [18, 107, 147]. To further reduce Pt loading, researchers have synthesized Pt nanocatalysts using atomic layer deposition [148] or nanostructured thin membranes with a loading of 0.1 mg cm^{-2} [149]. As a result of these findings, research has shifted away from the thickness and cost of electrodes to the uniform distribution of catalyst particulates. Furthermore, the study of catalyst loading limitations is also important in which the reduction in Pt loading from 1.1 to 0.2 mg cm^{-2} in both anodic and cathodic electrodes can lead to significant decreases in anode potential but no obvious changes at the cathode, indicating that HOR can significantly influence EHC performance [138]. Moreover, relatively few studies have been conducted in the optimization of Pt catalyst ratios in anodes and cathodes as well as the exploration of catalyst durability under high pressure. Researchers [147] have also detected that the equipotential line in thick membranes was prone to dehydration at 0.08 A cm^{-2} and reported that at such low current densities, the small overpotential of electrode reactions is difficult to measure if the amount of Pt loading in CLs is large. As a result, the Pt loading of both anode and cathode CLs was regulated to as low as 0.05 mg cm^{-2}. Bubble formation (i.e., super saturation of bubbles detaching from the CL) can also affect the CL stability of EHC cathodes and high-pressure hydrogen generation can lead to mass activity losses [150]. The formed bubbles can further block electrode surfaces to prevent catalytic reactions and cause stress on large electrode surfaces to degrade overall EHC performance [151].

In terms of carbon supports for EHC catalysts, the corrosion of carbon supports is not considered because the voltage required to drive reduction and oxidation reactions is by definition zero (except for a small overvoltage). However, characteristics such as high surface area, ability to maximize triple-phase boundaries through porous structures, good metal catalyst support interactions, high electrical conductivity and good water management need to be considered in the selection of carbon supports. Based on this, nano-carbon supports such as nanotubes, fibers and aerogels are promising replacements for traditional carbon supports for electrocatalysts and can be effectively used to reduce Pt loading. The alloying

of Pt catalysts with non-Pt group metals such as ruthenium, rhodium, iridium and osmium is also a promising strategy to decrease costs. And although the oxygen reduction reaction (ORR) demands high Pt catalyst loadings, there are still many reports for HER or HOR catalysts. Therefore, the holistic analysis of the catalytic activities of a single catalyst based on all reactions in a hydrogen electrode is important.

To further ensure the low loading of Pt, nanostructured CLs for MEAs in industrial production also need to be studied. For example, HyET hydrogen and NREL performed the X-ray fluorescence mapping and electrode structure characterization of HyET-produced electrodes for quality evaluation [96] and found that high-pressure environments can lead to the obvious destruction of CLs. Scanning electron microscopy and transmission electron microscopy also showed the degradation of CLs and the increased agglomeration of Pt nanoparticles at higher pressures. Therefore, the structural design of CLs plays a decisive role in durability [152]. Mass transport can also be affected by damages to catalyst structures under high-gradient pressures; however, Kim et al. [153] suggested that special pressure-resistant designs such as an inverse-opal-structured electrode (with a porous structure that can withstand high pressures and improve mass transfer and water management in CLs) can alleviate this issue. As for uneven reaction rates in anodes and cathodes, Taylor et al. [154] proposed that the optimization of Pt distribution and gradient loading in CLs is an effective solution. Here, these researchers showed that electrodes with a gradient design (Fig. 6b) were beneficial for the conduction of protons and the transport of different species such as gases or liquid water in which corresponding results revealed that the proper gradient distribution of Pt can effectively improve EHC performance, especially in areas of high current density, and significantly enhance mass transfer inside electrodes. Debe et al. [155] also reported that NSTF with an ordered microstructure can realize the separation and the order of electrons, protons and mass transfer channels to enable the improvement in catalyst utilization rates in electrodes and reduce the amount of Pt required. Moreover, carbon nanotube arrays as ordered catalyst carriers can also display high mechanical strength and conductivity; however, the corresponding stability is inferior water removal capability at low temperature [156]. Furthermore, metal oxides such as TiO_2, WO_3 and NbO_2 can reportedly replace carbon carriers in which the design principle of the interface between the CL and the membrane is to increase adhesion and therefore improve cell durability. Other studies

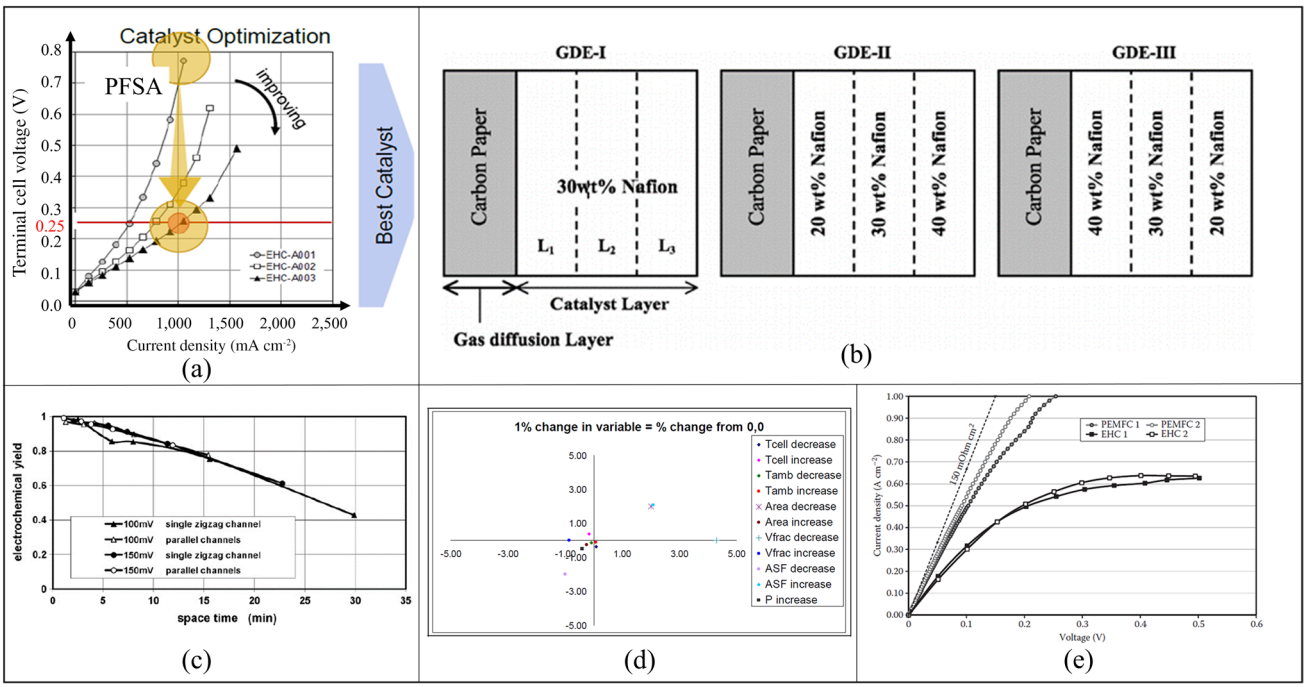

Fig. 6 (**a**) Performance of catalysts developed by Giner ELX Inc. Reprinted with permission from Ref. [82]. Sources from the US Department of Energy. (**b**) Schematic of GDEs based on CLs with uniform and graded Nafion content: GDE-1 (30 wt% Nafion), GDE-Il (20/30/40 wt% Nafion) and GDE-I1l (40/30/20 wt% Nafion). Reprinted with permission from Ref. [190]; copyright of The Electrochemical Society. (**c**) Electrochemical yield versus space–time for two types of gas distribution plates (cell voltage = 100 and 150 mV, $T = 298$ K). Reprinted with permission from Ref. [125]; copyright 2008 Elsevier B.V. (**d**) Baker diagram movement. Reprinted with permission from Ref. [111]; sources from the US Department of Energy. (**e**) Graph showing exemplary IV curves of identical MEAs testing hydrogen pumping performances in an EHC compression cell setup and in a PEMFC measurement setup. Reprinted with permission from Ref. [84]; copyright of CRC Press

have also focused on CL designs [157] based on the shape of flow fields [158, 159]. More significantly, Giner ELX Inc. was able to enhance catalytic performances by threefolds at 1000 mA cm^{-2} (Fig. 6a) [82]. As for the design of nanostructures on CLs, ordered and gradient designs can be used in anodes to increase the three-phase interface of reactions to further optimize anodic water management and durability whereas proper high-pressure structural designs in high-pressure cathodes can reduce CL damage. In addition, researchers have suggested that the substitution of metal oxides for carbon can enhance adhesion between CLs and membranes [160, 161]; however, metal oxides can also offer high electrochemical stability and high surface areas, and mechanical stability and durability. To achieve distribution uniformity, EHCs also require a high degree of rigor in the spraying process in which plasma sputtering and electrodeposition methods are promising in the development of highly efficient catalyst systems that can deliver good performance and stability with long-term durability.

In actual application, hydrogen usually comes from coal gasification and methane reforming. Therefore, hydrogen is always mixed with small amounts of CO and CO_2 that can poison catalysts in EHCs and decrease energy conversion efficiency in which small amounts of CO can be adsorbed onto Pt catalyst surfaces and compete with hydrogen adsorption to reduce the electroactive area of Pt. Here, Ru can be added to Pt catalysts to improve CO tolerance [124]. Based on this, Tokarev et al. [162] developed a CO adsorption model using the density functional theory to study CO tolerance capacities in which obtained experimental results showed that the adsorption energy of Pt_2Ru alloy was higher than that of $PtRu_2$. These researchers also found that CO was readily adsorbed at the edge of Pt and that the (110) surface (with a small coordination number) of Pt atoms adsorbed CO stronger than the (111) surface. They were also able to use Ru to purify hydrogen from a mixture of methane and hydrogen. In another study, Kim et al. [163] prepared an Ir/C electrocatalyst to remove CO_2 and compared its performance to that of traditional Pt/C catalysts. Here, these researchers reported that the exchange current density of the Ir/C catalyst treated at 300 °C (0.059 mA cm^{-2}_{SSA}) was larger than that of commercial Pt/C (0.043 mA cm^{-2}_{SSA}) and that through CO_2 stripping analysis, the performance of the Ir/C catalyst was found to be unaffected by CO_2 as demonstrated by the disappearance of the electrochemical desorption peak. To further avoid catalyst poisoning, MEMPHYS reported that catalysts can be renewed by using O_2 or O_3 in which O_3 is a better choice due to its quick speed. However, the addition of O_2 or O_3 requires a second-stage EHC stack system to obtain pure hydrogen and maintain hydrogen output flows constant [21]. Overall, the addition of Ru and Ir to form Pt alloys can effectively inhibit CO adsorption and intake strategies should consider the addition of small amounts of O_3 and O_2 to oxidize CO in the consideration of the cost and complexity of catalyst preparation.

In general, HER kinetics is slower than HOR kinetics and more attention needs to be paid to the enhancement of HER [123] in which HER has received great attention as a half reaction of electrolytic water due to its slow kinetics [164, 165]. However, challenges remain in the development of nanocatalysts to improve HER performance and current research on HER is mainly focused on Pt-based electrocatalysts, single-atom Pt catalysts, Pt-based alloys and non-Pt catalysts. However, more attention needs to be paid to the exploration of low-Pt or even non-Pt-based electrocatalytic materials to achieve low-cost, highly active and sustainable electrocatalytic materials for HER [166–168].

Although Pt-based catalysts are currently the main catalysts for HER, they also possess inherent problems mainly involving high prices and poor stability. Here, several strategies have been proposed to address these issues, including the downsizing of Pt to single-atom catalysts (SACs) [169] and the formation of alloys [170], all of which can significantly enhance catalytic performance by modifying catalyst surface hydrogen adsorption behaviors. Despite this, SACs possess relatively low-density active sites as well as an undesirable tendency toward aggregation. In addition, the preparation of noble metal-based alloys is a complex process in which many of the proposed bimetallic structures tend to change during reactions [171]. Therefore, the design of alloy catalyst atomic arrangements by using powerful characterization methods such as in situ spectroscopy is necessary. Furthermore, poor interfacial design strategies can lead to metal segregation and diffusion during long-term operation, meaning that the durability of Pt-based catalysts in EHCs is an issue that requires further research. Based on general physical and chemical properties, various earth-abundant and non-precious transition-metal-based compounds [layered transition-metal dichalcogenides (MoS_2 and WS_2), transition-metal phosphides, sulfides, nitrides, etc.] have also been widely studied as promising electrocatalysts that are expected to replace noble metals in water electrolysis applications. And with inspiration from the structures and compositions of nitrogenase and hydrogenase, researchers have also exploited a series of metal sulfides as efficient electrocatalysts for HER [172], which is a profound achievement in the field of non-noble metal HER electrocatalysts.

As for MoS_2 and WS_2-based materials, several designs involving nanoscale catalysts have been proposed to enhance catalytic activity based on instructional studies on active sites and semi-conductive natures in which as compared with original bulk materials, nanostructured [173, 174] and porous structured [175] materials were found to usually possess larger specific surface areas with higher densities of active sites. To further improve electrical contact in active sites, researchers have also proposed several methods such as doping with

suitable heteroatoms into base material lattices and the coupling of base materials with conductive species such as carbon nanotubes and graphene. Different from carbides and nitrides with relatively simple crystal structures (e.g., face-centered cubic, hexagonal close-packed or simple hexagonal), the crystal structures of phosphides are based on trigonal prisms due to the large radius of phosphorus atoms (0.109 nm) in which metal phosphides tend to form more isotropic crystal structures rather than the layered structures observed in metal sulfides [176]. And as a possible result of this structural difference, metal phosphides possess greater numbers of coordinatively unsaturated surface atoms than metal sulfides [177–179].

Many other materials have also shown great potential in HER catalysis, such as CoP [180], FeP [181], MoP [182, 183], MoN [184], WC [185] and $MoSe_2$ [186], and overall, the design of catalysts has attracted special attention in the field of HER in the attempt to decrease or even replace rare noble metal electrocatalysts.

4.3 Flow Field and Gas Diffusion Layer

The flow field and the GDL of EHCs can affect the distributions of mass transportation and temperature and are crucial components in EHCs.

4.3.1 Flow Field

The main role of flow fields is the accommodation of mass distribution and transportation in porous electrodes with minimal pressure drops in which careful designs are required for flow fields at EHC anodes. Alternatively, porous electrodes can produce high-pressure hydrogen gas directly in EHC cathodes without the existence of a flow field.

Currently, most existing flow fields used in EHCs are similar to those used in PEMFCs and include single serpentine [125, 140, 187], pin-type (grid-type) [20] and parallel channel types. Here, Casati et al. [125] suggested that between single serpentine and parallel channel flow fields, the parallel channel flow fields showed slightly higher hydrogen recovery rates but low values of space–time, indicating the influence of different shapes in flow fields on performance under different pressures (Fig. 6c). In addition, Shimpalee et al. [188] reported that both the channel-land (rib) dimension and the shape of flow fields can have significant influences on the flow rate, the water removal, the pressure drop, the mechanical stability and the temperature distribution in which through the hydrogen void fraction in cathodes and the sensitivity study of the pressure drop, corresponding flow field channels can be determined. Bloomberg et al. [111] also used the variables involved in determining the location on a baker diagram [T_{cell}, T_{amb}, the pressure, amps per square foot (ASF), the void fraction and the channel area] to construct a spreadsheet to determine movement on the baker diagram as a function of individual parameters (Fig. 6d). Furthermore, Analytic Power Corp. reported that the main flow patterns found in their experiments were on the border of the bubble flow and the plug flow, which led to a decrease in the void fraction from 7.620 to 3.810 mm in which the channel depth was set to 0.127 mm and a higher current density of 350 A cm^{-2} as compared with 300 A cm^{-2} was selected based on expected performance improvements from their proposed design. Here, these researchers settled channels wider than lands with a ratio of 2 to 1 and reported that this ratio of land-to-channel can decrease pressure drops across the flow field and improve the water removal from the GDL to result in more contact area between reactants and the GDL as well as a reduction in total voltage loss [189]. Interestingly, Bessarabov et al. [84] reported that in two duplicate datasets obtained from the same membrane and catalyst, an expected linear trend was observed in a PEMFC whereas an EHC showed greater limitations above a certain current density followed by a leveling off, which suggested that the limitation was caused by the environment of the MEA (Fig. 6e).

4.3.2 Gas Diffusion Layer

GDLs are porous structures that play critical roles in EHCs in which common examples include carbon paper (e.g., Sigracet, Freudenberg, Toray) made by pressing carbon fibers and carbon cloth (e.g., ELAT) made by weaving carbon fibers and porous metal. GDLs should possess high electric conductivity, great mechanical strength, appropriate porosity and good chemical stability for high-performance EHCs. One function of GDLs is to support CLs and accommodate the diffusion of reactants, water, heat and electrons in which for the support of CLs, pressure differences between anodes and cathodes can lead to distortions on MEAs and flexible GDLs can play an important role in contacting CLs to avoid damage. GDLs can also facilitate diffusion across the channels of bipolar plates and CL membranes based on surface area and porosity in which increased surface areas of GDLs can increase the current between catalyst sites in MEAs and current collectors. As for the diffusion of water, GDLs can also handle the moisture control of EHCs in which GDLs can not only remove water outside CLs from the anode to prevent chamber flooding, but also maintain the wetting of CL surfaces to improve conductivity throughout the membrane. Moreover, GDLs also play an important role in the control of heat transfer during EHC operations. And based on all of this, the rational design of the configuration and coating of GDLs is critical to EHC performance.

Because of the obvious pressure difference between anodes and cathodes in EHCs, single and multi-layer porous metal materials [191, 192] as well as matched double GDLs (porous metal and carbon cloth) with carbon cloth [193] can be used as GDLs to support membranes on the anode

side whereas for the cathode side, highly elastic materials can be used to provide shock absorption and supplement membrane deformation to inhibit the increase of contact resistance between GDLs and CLs.

As examples, a graded GDL with a porosity gradient possessing fewer numbers and larger sizes of holes as well as softer materials and rougher surfaces from the inside to the outside was used for the anode side by Panasonic Ip Management Ltd. (Fig. 7a) and Analytic Power Corp. considered a sintered titanium cell support on the anode side of an EHC to increase the percentage of holes in which the resulting active area exposed to reactant hydrogen was ~ 25% because of the porous support of the metal electrode [111]. These researchers also investigated porous metal supports that can be manufactured to be less than 0.127 mm thick and with up to 80% open ratios (Table 4) but reported that suitable corrosion-resistant materials were not found. As for double GDLs, porous metals can play the role of flow fluid and carbon cloth can be used to remove direct mechanical damage between porous metal and membranes. In terms of materials used in GDLs, sintered Ti is generally expensive and special designs with anisotropic pore sizes are even more costly. In addition, titanium can be oxidized by water and formed TiO_2 layers are not conductive. Analytic Power Corp. also found that TiN coating layers used to protect Ti plates can be oxidized in EHC cell environments. Alternatively, researchers from both LANL and Giner Inc. [111] have suggested that optimal materials for electrode support screens in EHCs should be either molybdenum or niobium expanded metals. Toray Industries also investigated the effects of porous metal characteristics in EHCs including different thicknesses, porosity and shapes (Table 5) [85], and although many researchers have mentioned the use of porous metals in EHCs in their research, no detailed discussions have been provided.

Other than the development of GDL materials, the application of effective surface coatings is another important method to improve water management capabilities. For example, Lee et al. [193] used a low-cost fabrication method to prepare a hydrophobic coating consisting of Nafion and O-CNTs for porous GDLs to overcome anode flooding and reported that as compared with an EHC using an untreated GDL that could not recover from flooding at ambient temperature, an EHC using the GDL modified by O-CNTs and Nafion recovered completely in ~ 100 s. The use of high-elastic materials on the cathode side can compensate for the deformation of membranes and thereby reduce contact resistance between CLs and GDLs and provide shock absorption in which the degradation of EHC cell performance and damage to GDL microstructure are mainly caused by mechanical degradation [195].

Compression pressures can also strongly influence the properties of current collectors, CLs and bipolar plate interfaces, thereby affecting overall EHC performance in which optimal compression ratios can allow for maximized EHC performances. And because gas permeability decreases nonlinearly with GDL compressed thickness, differences in permeability can experience orders of magnitude in variation between compressed (250 μm) and uncompressed (380 μm) GDL sections. In addition, mass, heat and charge transport phenomena in non-uniformly compressed GDLs can considerably differ from those in uncompressed GDLs [196]. Here, an FEM model was adopted in many studies to obtain the properties and real shapes of elastically deformed GDLs as a function of clamping pressure and a species transport model was also applied to deformed GDLs to predict species distribution and cell performance [197, 198], thus allowing for greater insights into the effects of GDL compression on interfacial contact resistance, species transport and EHC performance.

In terms of GDL materials, common materials used in commercial GDLs contain carbon paper, carbon cloth or carbon felt. Here, comparisons of resistance and structural stability at high pressures revealed that increased load cycles can cause the gradual consumption of resistance and the cracking of fibers in carbon paper and carbon cloth whereas the stability of carbon felt performed much better in terms of electrical resistance and microstructure due to its tortuous and thick fibers (Fig. 7b, c). Moreover, the influence of GDL compression on carbon paper and carbon cloth was found to be relatively large under high current densities [194, 199]. Based on this, Giner ELX LLC proposed a mixture of chopped carbon fibers, milled carbon fibers and PVDF powders that was able to maintain above 90% original thickness under a pressure of 13.789 MPa [200]. Despite this, most studies concerning GDLs have been based on the clamping force of fuel cells and few studies have focused on the effects of high-pressure gas on GDL compression.

Overall, future research should focus on the exploration of new GDL materials such as Al/Mg/Si alloys and polymer-coated materials. In addition, the investigation of expanded metal screen electrode supports and metal-felt-based GDLs should be addressed in which metal felts can be effectively coated with imide or siloxane polymers. However, metal felts are designed for high differential pressures and corresponding membranes or GDLs may be pressed into channels under high-pressure situations. Therefore, the maximum pressure on EHC cathode sides is restricted.

5 System of EHCs

5.1 Thermal Management

An EHC is a fundamentally isothermal compressor in which temperature remains in principle constant during

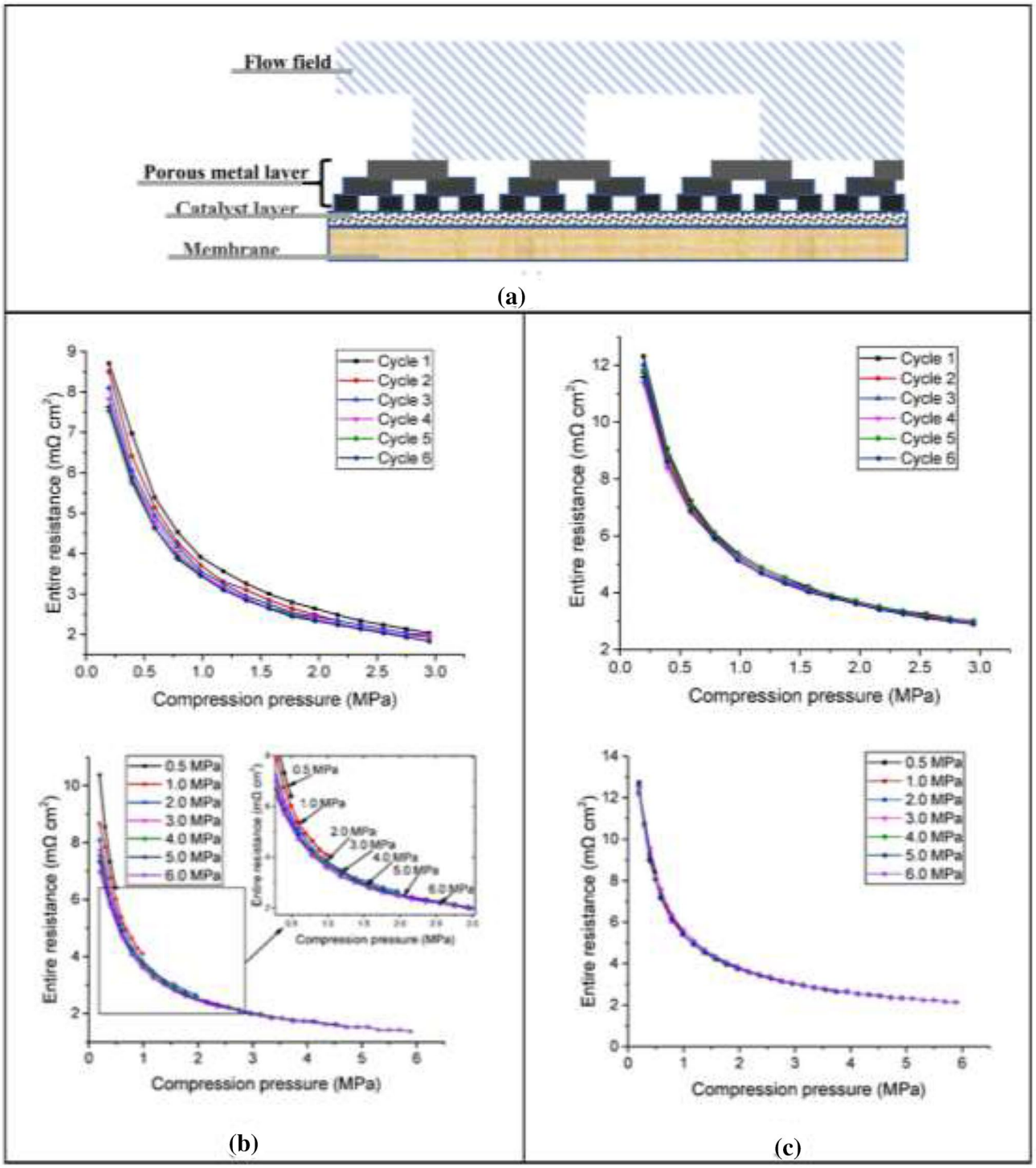

Fig. 7 (**a**) A graded GDL with a porosity gradient developed by Panasonic Ip Management Ltd.; (**b**) cyclic and steady load effects on cell assembly with Tenax cloth: cyclic and steady load effects on resistance. Reprinted with permission from Ref. [194]; copyright 2018 Elsevier B.V. (**c**) Cyclic and steady load effects on cell assembly with Freudenberg carbon felt: cyclic and steady load effects on resistance. Reprinted with permission from Ref. [194]; copyright 2018 Elsevier B.V

Table 4 Expanded metal screen alternatives. Reprinted with permission from Ref. [111]. Sources from the US Department of Energy

Dexmet product code	1.3NB3-020F	5NB5-031F	10NB10-050F
Base metal thickness (mm)	0.033	0.127	0.254
Material	Niobium	Niobium	Niobium
Strand width (mm)	0.076	0.127	0.254
LWD (mm)	0.508	0.787	1.270
Open area (%)	50	50	31

compression; however, Corgnalea et al. [80] reported that EHC stacks can potentially generate 4.75 kWh kg^{-1} of heat at 2.5 A cm^{-2}. Based on this, proper thermal control is necessary to maintain constant performance and avoid temperature-induced variation in the cells of EHC stacks in which air convection cooling and liquid cooling are two main strategies. In addition, if cooling requirements are low at low current densities, convective air-cooling can also be used. As for single cells and short stacks, metal endplates can also act as radiators to dissipate excess heat from cells. Here, because of the existence of a parabolic temperature distribution in EHC stacks with the hottest part in the middle in which heat is transported to adjacent cells, the external heating of end plates can be used to increase external temperatures before operation to allow the temperature of central cells to be the lowest. And although external heating cannot correct the distribution of parabolic temperature during operation, it can affect the temperature offset of the overall stack profile and therefore increase middle cell temperatures as well. Imprecise designs can further lead to extreme temperature differences that can reach ten degrees between the hottest middle cell and the coolest external cell. However, as the number of cells increases, heat loss through the endplates remains almost the same whereas the demand for heat rejection increases proportionately. Sustainable Innovations also studied thermal management solutions for EHC stacks [201] and based on the assumption that heat was uniformly generated over the active area, a convection coefficient was estimated for free convection in a standard multi-cell stack in which the convective surface area of their stack was nearly 20 cm^2 with the exposed ends of the cells used for cooling. As a result, these researchers reported that the protruding cells in their stack increased the effective convective surface area by nearly 17 times (Fig. 8a). Moreover, this company constructed thermal models with both thick and thin membranes for EHC stacks and found that temperatures can vary greatly with or without fins at different current densities (Fig. 8b). Aside from natural convection air-cooling, the circulation of cooling water is another common method to deal with thermal issues as well as provide humidification to cells. Concentration gradients can also be created through the addition of solutes (e.g., sugar) to cathode water to drive water formed in the anode compartment to the cathode. Despite these solutions, corrosion remains an issue that has not been resolved [111]. In addition, although proton conductivity, water management and back-diffusion are all affected by the temperature of EHC systems, no comprehensive mathematical models have been provided in literature focusing on the simultaneous simulation of these aspects in EHCs. Here, a model to predict the required level of thermal control in EHC systems is greatly beneficial to the avoidance of unstable and detrimental off-spec operating conditions.

5.2 Water Management

Water management is a key factor in the performance of EHCs because of the water content dependency of membrane conductivity, particularly for low-temperature EHCs. In addition, excess water can cover reaction sites on electrodes and hinder reactant flows through flooding to also affect EHC performance. Overall, water transport in EHC membranes occurs through three mechanisms, including electro-osmotic drag, concentration gradient induced diffusion and pressure gradient induced convection.

In terms of PEMFCs, modeling results have shown that performances can be improved by increasing differential pressure between cathodes and anodes to result in the increase of water back-diffusion across membranes [202]. In addition, several water transport models have been built based on PEMFCs [203, 204]. However, the scale of applied high-pressure differentials in PEMFC models may generate different predicted values from EHC physical models. And although Kusoglu et al. [205] discussed the internal balance between chemical and mechanical forces in the

Table 5 Characteristics of porous metal for Toray tests. Reprinted with permission from Ref. [85]. Sources from the Japan The New Energy and Industrial Technology Development Organization

Test number	Thickness (mm)	Porosity (%)	Shape	Laser microscope image (μm)
A	1.3	31.9	Particle (size: 100 μm)	25
B	1.1	49.1	Particle (size: 100 μm)	50
C	0.58	67.2	Fibrous (size: 20 μm)	20
D	0.01–1	10–20	Etch holes	No data

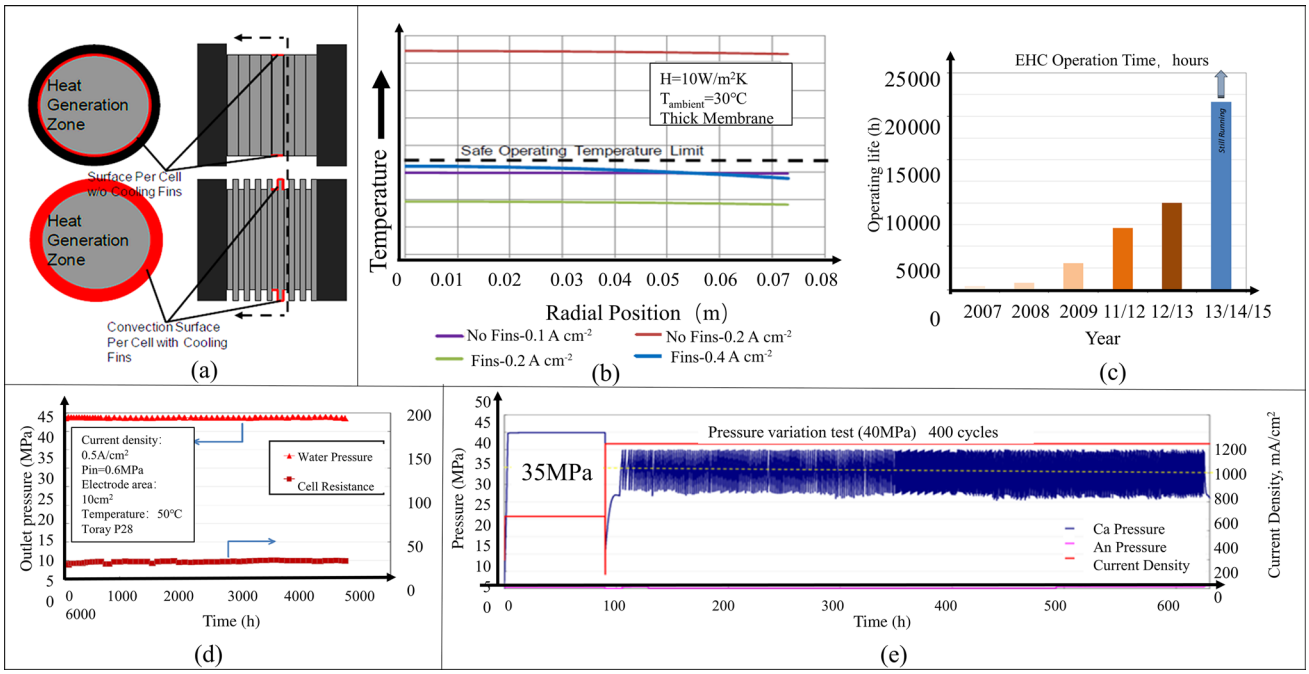

Fig. 8 (**a**) Thermal management model for stacks with cooling fins as developed by Sustainable Innovations for NASA. Here, cooling fins can significantly increase convective surface areas from 3 to 50 in^2. Reprinted with permission from Ref. [201]. Sources from the US Department of Energy. (**b**) Thick membrane thermal modeling results in which the addition of cooling fins can allow thick membrane EHCs to run at current densities 4 times greater than EHCs with no fins. Reprinted with permission from Ref. [201]. Sources from the US Department of Energy. (**c**) Over 22000 h of endurance testing demonstrated in a scaled-up EHC cell in which operating hours have increased by almost an order of magnitude since the start of the program. Reprinted with permission from Ref. [201]. Sources from the US Department of Energy. (**d**) Durability evaluation under high pressure; (**e**) pressure variation experiment by using P28 developed by Toray Industries. Reprinted with permission from Ref. [85]. Sources from Japan, The New Energy and Industrial Technology Development Organization. (**f**) 5-cell EHC stack life chart. Reprinted with permission from Ref. [85]. Sources from Japan, The New Energy and Industrial Technology Development Organization

determination of the water content and the *d*-spacing of water domains in PFSA membranes and showed that direct hydrostatic pressure confinement can reduce the water content by using small-angle X-ray scattering (SAXS), more experiments are needed to verify that decreases in the water content become less significant at 25 MPa. Casati et al. [125] also showed that the better control of the membrane hydration degree can be achieved by adopting variational operating conditions instead of galvanostatic ones and Onda et al. [187] found that both hydrogen flow relative humidity and current density distribution decreased along the channel direction during EHC operation because of unbalanced contributions from two main water transport mechanisms across the membrane (i.e., back-diffusion and electro-osmotic drag). This uneven distribution of transport mechanisms can also lead to localized membrane dehydration, which can increase local resistances. In a further study, Sdanghi et al. [206] developed a pseudo-2D model to prove that the stability of current density distribution strictly depended on the local water content of membranes but that contrary to PEMFC cathodes, no constant resupply of water was produced at the cathode side in EHCs in which the amount of water at the EHC cathode from electro-osmotic drag may not be enough to humidify the membrane, especially at low current densities and high temperatures. Therefore, EHCs need to be improved based on other water management strategies (internal humidification) due to the inlet of dry hydrogen aside from the strategy of humidifying inlet hydrogen.

Researchers have also reported that the use of internal humidifiers in cathode end plates is an improved design [207] as compared with humidification achieved through bubblers and that internal humidifiers can be used at both anode and cathode sides [83]. Unfortunately, water convection as caused by pressure gradients is usually ignored in these studies with more attention being paid on concentration gradients [147]. Analytic Power LLC also developed a hydraulic cathode that circulated water through the compressor cathode to cool the cell and humidify the membrane, thus accommodating the use of dry hydrogen in anodes and avoiding the fundamental problem of anode flooding, which is a principal challenge in prior designs. In this study, the diffusion of water was also accelerated through the addition

of a substance to create a concentration gradient in the water [111].

Aside from the humidification of EHC devices, Giner Inc. reported the development of a membrane called WaMM in which the composite membrane combined an ionomer with an electrical conductor composed primarily of carbon nanotubes that enabled improved water retention capacities in which water can be fed to one side of the WaMM and permeate through the membrane to the adjacent PEM, thus allowing water in the PEM to be self-replenishing due to the creation of a concentration gradient between the WaMM and the PEM. As a result, the developed WAMM with a high water flux (more than 0.10 g min^{-1}) can display 1.0 S cm^{-1} of through-plane conductivity. And as assembled in a bipolar stack configuration, the WaMM experienced insignificant cell voltage losses of less than 6 mV $cell^{-1}$ at a current density of 1000 mA cm^{-2} [133].

5.3 Models of EHC

Models of EHCs can allow for the analysis of influences from design parameters including electrode thickness, porosity and catalytic activity on cell performance. For example, because transport and electrochemical phenomena occur perpendicularly to the MEA direction in EHCs and significant variations in water and hydrogen concentration can occur as binary mixtures that flow along gas channels, 1D models cannot adequately describe the transport phenomena. Therefore, Nordio et al. [78] developed a 1D + 1D model of EHCs based on MATLAB by taking into account the changes of total pressure, total flow and hydrogen concentration in anodes and cathodes in which through the Butler–Volmer equation, simulations with different hydrogen concentrations for mixtures at different voltages can be performed. Here, a diffusive membrane model approach along with steady-state operations and gas phases was chosen in this model to treat the main system and therefore enabled the model to predict the polarization curve and purity of outlet hydrogen. Water content, pressure and back-diffusion effects on EHCs are also important research topics in which experiments at higher pressures and temperatures are needed to verify the accuracy of corresponding models. Here, Sdanghi et al. [208] developed a pseudo-2D model that was validated through comparison with obtained experimental data that can take into account both overall mass and energy balance in EHCs as well as heterogeneity in relative humidity along gas distribution channels. And by using this model, these researchers proved that the stability of current density distribution strictly depended on the local water content of membranes and was able to provide good predictions for both current density distribution and relative humidity at anode outlets under different current densities. These researchers also found based on this model that unstable operating conditions can occur if low relative humidity hydrogen was fed to EHCs due to water consumption at the cathode side. Sdanghi et al. [209] also investigated the uneven contribution of electro-osmosis flow and back-diffusion of water across membranes along with a series of parameters including humidity, temperature, membrane thickness, outlet pressure and the stoichiometric ratio in order to optimize overall efficiency.

Bampaou [210] also developed a zero-dimensional steady-state EHC model (temperature—up to 343 K; pressure—15 MPa) to calculate overall voltage by taking into account the Nernst voltage, ohmic loss and activation overpotential using commercial software (AspenPlus™). These researchers also used this model to evaluate required power and cooling loads based on water management and were able to quantify the extent of water flooding issues and liquid water that should be removed. In a further study, Rahbari et al. [211] combined working conditions and used molecular simulations and thermodynamic modeling to study the phase coexistence of H_2O–H_2 systems based on temperatures ranging from 283 to 423 K and pressures from 1 to 100 MPa. A thermodynamic model was also proposed with results that agreed with previous experimental data [112, 140]. Toghyani et al. [16] also compared a compressor with an ejector and observed that the performance of the ejector recirculation system was similar to that of the EHC recirculation system and that EHC recirculation system efficiency was higher than that of a mechanical compressor at low current densities (< 0.1 A cm^{-2}). These researchers also reported that at intermediate and high current densities, the performance of the ejector was better than that of the EHC because the operation of PEM fuel cells at higher current densities can lead to increases in parasitic power. Furthermore, this study focused on anode recycling systems and evaluated the effects of general parameters on PEMFCs, including operating temperature, pressure, relative humidity, the number of cells and active area of PEMFC stacks with EHCs.

5.4 Performance Testing of EHC Stack

The durability and voltage consistency of individual cells are key considerations in the design of EHCs in which the endurance of EHC cells is considered to be a critical parameter in life-cycle costs. Here, Fuel Cell Energy Inc. has devoted significant attention to the durability testing of EHCs [201] in which a developed single-cell system showed significant enhancements to endurance with operational time increasing from 6000 to 10,000 h at an elevated current density of 750 mA cm^{-2} from 2012 to 2013. Endurance testing further shifted in 2014 and 2015 from hardware with 81 cm^2 (a 30-cell stack with endurance testing for more than 1600 h at 31.03 MPa) to 185 cm^2 with one cell operating for more than 22000 h with a hydrogen recovery rate above 95%. To

further demonstrate the robustness of their EHC, stress testing of similar single-cell stacks was also simulated, which underwent over 1000 pressure cycles with minimal losses in cell performance. And due to the efforts by Fuel Cell Energy Inc., the durability of their EHC increased by several orders of magnitudes from 2007 to 2015 (Fig. 8c). Recently, Toray Industries also verified that their products can show durability above 5000 h at constant output pressures between 40 and 45 MPa without damage to cell components (Fig. 8d) in which in pressure variation tests between 30 and 40 MPa, no damage to MEAs or to cell components was found after 400 cycles (Fig. 8e). Despite this, Toray Industries also observed a worse phenomenon occurring in multi-cell EHC stacks in which in a 5-cell stack for example, the 5th cell was consistently almost twice the voltage of other cells. In addition, voltages were not evenly distributed among the cells in the 5-cell stack EHC, which ranged from 50 to 700 mV (Fig. 8f). And although the report did not mention the harm of this voltage inconsistency, the lifespan of individual cells may be threatened, which will subsequently affect the entire stack in a multi-cell EHC [85]. Furthermore, through the continuous modification of one design and improvements to fabrication and system controls, researchers were able to obtain a uniform cell-to-cell potential in a 30-cell stack across every cell in which within the 30-cell stack, variations were over 70% lower than previous stack designs after 4 years of improvements, suggesting that individual cells need to be designed carefully. In 2006, Barbir et al. [18] also evaluated performances using an EHC for the recirculation of hydrogen in a 10-cell stack and achieved satisfactory and stable results.

The current parameters and application of EHCs are shown in Table 6.

6 Conclusions, Challenges and Prospects

The issue of low hydrogen volume density in storage needs to be resolved for the future large-scale application of hydrogen as a widespread renewable fuel to replace traditional energy sources in which hydrogen compression is a direct approach. Here, commonly used hydrogen compressors can be divided into mechanical compressors and non-mechanical compressors in which mechanical compressors include widely used reciprocating and diaphragm compressors as well as novel ionic liquid compressors whereas non-mechanical hydrogen compressors include cryogenic compressors, adsorption compressors, metal hydride compressors and electrochemical hydrogen compressors. Based on this, this review has presented the advantages and disadvantages of these different types of compressors. In terms of EHC systems, this review has provided a comprehensive overview with discussions on key components and system management strategies. Here, EHC membranes require high proton conductivity, good mechanical integrity (i.e., durability, strength) and low hydrogen back-diffusion and major membranes explored include PFSAs, hydrocarbon membranes, protonic ceramic membranes and ion-solvating polymers, all of which have been described in detail in terms of both the current research status and existing challenges. As for CLs in EHCs, structural designs can reduce catalyst usage and potential failure in high-pressure situations whereas the reasonable design of three-phase interfaces can improve CL activities as well as mass transfer. And in terms of actual catalysts in EHCs, various metal catalysts can be used to purify hydrogen mixtures to reduce Pt inactivation and similar to the research direction in fuel cells and water electrolysis systems, the development of low-Pt and non-Pt catalysts remains the main goal in the future. With regard to flow fields and GDLs, the distribution of water and gas in flow channels and GDLs is a critical issue that is connected to geometric design, support material property and coating material in which the further exploration of high-pressure differentials in channels and GDL designs remains lacking. In addition, heat generation from cell resistance and excess driving voltage in large-scale EHCs also need to be reduced through air-cooling or liquid cooling methods to achieve thermal management in which models to predict the required level of thermal control to evaluate unstable or even detrimental off-spec operating conditions are necessary. Water management is also a critical focus in EHCs in which anode humidification alone is insufficient and requires water generation at cathodes as well at low current densities and high temperature. Here, main approaches include gas humidification, water admission in both electrodes and wetting coatings. Moreover, because the working principles of EHCs are different from that of PEMFCs, high-pressure differences can lead to different predicted values in physical models, which will require further exploration through experimental testing. In terms of the overall performance of EHCs, durability and voltage consistency are vital determinants to evaluate the proper design of EHC stacks in which the design of active area, pressure, temperature and other factors can affect the results of performance tests.

Overall, the main challenges of EHCs can be summarized as follows.

1. The design of membranes that can determine the performance of EHCs in which back-diffusion and mechanical strength are two critical parameters remains lacking. To resolve this, operation conditions and policies (the temperature, the outlet pressure, the membrane water content and the inlet flow) need to be considered and optimal combinations need to be elucidated. Here, a simple method to decrease hydrogen back-diffusion and enhance mechanical strength is to increase membrane thickness. As for uneven pressure distributions in membranes, membrane packaging designs should be

Table 6 Performances and characteristics in the application of various EHCs

Author and Ref. (year)	Membrane electrode assembly (MEA)						Operating conditions					Performance in EHC
	Membrane (thickness)	Electrodes (active area)	Proton conductivity (S/cm)	Back-diffusion	Mechanical strength	GDL	Temp (°C)	Gas composition and P_{in} (MPa)	P_{out} (MPa)	Flow (Nm^3/h)	Applied voltage or applied current density	
Rohland et al. (1998) [212]	ETEK MEA Nafion 117	Pt, 2 mg /cm^2 (100 cm^2)	No data	24 °C: 0.08 ml/bar·min cm^{-2}; 70 °C: 0.27 ml/bar min cm^{-2}	No data	Metal felt matrix	24, 70	H_2; 0.1	4.3	0.04–5.7	100 mA/cm^2, 200 mA/cm^2, 350 mA/cm^2	Efficiency loss of 5%, at 350 mA/cm^2, 16 MPa at 24 °C, 4.6 MPa at 70 °C
Strobel et al. (2002) [112]	WL GORE MEA 6000 (40 μm); ETEK MEA Nafion 105(120 μm); ZSW MEA Nafion 115 (120 μm); ETEK MEA Nafion 117(200 μm)	Pt, A/C: 167μg/cm^2, 171μg/cm^2 (25 cm^2)	No data	(1) 1.85×10^{-7} cm^2/s (2) 2.44×10^{-7} cm^2/s (3) 2.56×10^{-7} cm^2/s (4) 2.10×10^{-7} cm^2/s	No data	No data	No data	H_2; 0.1	4.3–5.4	1–6	200 mA/cm^2	500 mA/cm^2 0.25V 1 cell 43 bar; 330 mA/cm^2 0.4V 1 cell 43 bar; 300 mA/cm^2 0.45V 3 cells
Lee et al. (2004) [107]	Nafion 115 (127 μm)	Pt, 0.4 mg/cm^2 (5 cm^2)	No data	No data	No data	No data	30, 50, 70	H_2–N_2–CO_2 gas; 0.1–0.3	No data	0.008–0.11	300 mA/cm^2	300 mA/cm^2, High purity: 97.39%
Analytic Power Corp (2006) [111]	Nafion117 (279 μm, 381 μm, 431 μm)	Pt, 0.5mg /cm^2/side (Irregular figure)	No data	No data	No data	Carbon paper supported GDL and a metal screen electrode	71	H_2	17.2	0.0468	200–1000 mA/cm^2	0.215 V@ 391 A/cm^2
Ibeh et al. (2007) [213]	No data	A/C: Pt, 1 mg/cm^2, Ru, 0.5 mg/cm^2; Pt, 1mg /cm^2 (25 cm^2)	No data	No data	No data	No data	20–70	H_2, H_2 in methane gas; 0.1	No data	0.009, 0.018, 0.036 mL/s gas mixture of H_2 and methane	190 mA/cm^2, 340 mA/cm^2	No data
Dale et al. (2007) [214]	No data	No data	No data	No data	No data	Cathode: a flexible graphite sheet	24, 35, 60, 70	No data	>6.3	No data	No data	No data
Gardner et al. (2007) [124]	Nafion115	Pt, 1 mg/cm^2, Ru, 0.5 mg/cm^2 (25 cm^2)	No data	No data	No data	No data	20	H_2–CO_2–CO gas; 0.5	No data	0.00195, 0.00375, 0.00495	240 mA/cm^2	Over 80% with 80% H_2 extraction
Perry et al. (2008) [139]	PA-PBI	Etek electrodes, Pt, 1.0 mg/cm^2	0.28 at 160 °C	No data	No data	No data	120, 140, 160	H_2–CO_2–CO gas; 0.1	No data	0.00450, 0.00564	200, 400, 800 mA/cm^2	The content of CO and CO_2 decreased obviously
Casati et al. (2008) [125]	Nafion117	Pt, 0.1 mg/cm^2 (50 cm^2)	No data	No data	No data	No data	20–70	H_2–N_2 gas mixtures	No data	0.00024–0.0048	35, 50, 100, 150 mV	No data
Onda et al. (2009) [187]	No data (80 μm)	No data	No data	No data	No data	Carbon paper (thickness: 200 μm)	60	H_2–N_2–CO_2 gas; 0.13	0.13	0.000228, 0.00228	0–50 or 500 mA/cm^2	No data
Nguyen et al. (2011) [123]	Nafion117 SPE	40 wt% Pt on a Vulcan XC-72 carbon carrier of large (250 m^2/g) (7 cm^2)	No data	No data	No data	A/C:Sigracet 10 bb carbon paper; Porous titanium porosity: 30%	23–70	H_2, H_2–N_2 gas; 0.1	No data	No data	200 mA/cm^2	No data
Grigoriev et al. (2011) [83]	Nafion 117 (183 μm)	Pt/C, 0.4–0.8 mg/cm^2 (25 cm^2)	No data	No data	No data	A/C:Sigracet 10 bb carbon paper; Porous titanium porosity: 30%	35, 55, 75	H_2, H_2–N_2 gas	13	0.01	200 mA/cm^2	No data
Yang et al. (2011) [133]	Membrane based on poly-2-vinylpyridinium dihydrogen phosphate (625 μm)	Pt, 8 mg/cm^2 (5 cm^2)	0.01 at 140 °C, The proton transport number :0.17–0.20	No data	No data	Toray carbon paper (TGPH-060, 10% teflonized)	120–180	No data	2.5	No data	No data	No data

Table 6 (continued)

Author and Ref. (year)	Membrane electrode assembly (MEA)						Operating conditions					Performance in EHC
	Membrane (thickness)	Electrodes (active area)	Proton conductivity (S/cm)	Back-diffusion	Mechanical strength	GDL	Temp (°C)	Gas composition and P_{in} (MPa)	P_{out} (MPa)	Flow (Nm^3/h)	Applied voltage or applied current density	
Buelte et al. (2011) [142]	PBI	Etek Pt, 1 mg/cm^2	No data	No data	No data	No data	160	H_2–CO_2 gas	No data	1.2 X the requirement for the hydrogen pumping current	200 mA/cm^2	No data
Sakai et al. (2013) [91]	$La_{0.9}Ba_{0.1}YbO_{3-\alpha}$, LBYb-91 (500 µm)	Porous Palladium	0.0042	No data	No data	No data	800	H_2	No data	No data	40 mA/cm^2	High chemical stability towards CO_2 and H_2O
Kim et al. (2013) [138]	GORE M815 series (15 µm); PBI/PA membrane (30 µm)	Pt/C, 1.1–0.2 mg/cm^2, 0.4–2.2 mg/cm^2; (25 cm^2, 10.24 cm^2)	No data	No data	No data	Sigracet 10BC with MPL, SGL Co.	160	Humidified H_2–CO_2 gas	No data	0.01308	800 mA/cm^2	80 mV at 800 mA/cm^2
Wu et al. (2014) [215]	SPEEK/ CrPSSA sIPN (100 µm)	Pt/C, Pt, 0.5 mg/cm^2, (1.9 cm^2)	0.08–0.1	No data	No data	No data	80	Humidified 80% H_2-20% CO_2 gas	No data	0.00096	No data	Energy efficiency of 30%
Lipp et al. (fuel cell energy) (2014) [135]	No data	No data	No data	No data	No data	No data	No data	H_2, 0.1–14	83	0.06	No data	No data
Moton et al. (2014) [216]	Nafion® (127 µm)	Pt, 0.1 mg/cm^2 (200cm^2 –400cm^2)	No data	No data	No data	Anode: Porous titanium, thickness: 300 µm	70	H_2, 0.35	7–100	116–467	400 mA/cm^2, 1000 mA/cm^2	No data
PHAEDRUS project (2014) [217]	No data	No data	No data	No data	No data	No data	20,80	No data	100	0.93	No data	No data
DON QUICHOTE project (2014) [217]	No data	No data	No data	No data	No data	No data	20,80	No data	40	28	No data	No data
Huang et al. (2016) [218]	SPPESK (70 µm)	Pt/C, Pt, 0.5 mg/cm^2, (1.9 cm^2)	0.0338	No data	No data	(GDL, 35BC) with a micro-porous layer	40	Dry 25% H_2-75% CO_2 gas	No data	0.003	56.7 mA/cm^2	> 99.99% H_2; Energy efficiency: 35% at 60% H_2
Hao et al. (2016) [147]	Nafion®117 membrane	Pt/C, Pt, 0.2 mg/cm^2, (5.3 cm^2)	No data	No data	No data	A/C porous SUS316L, a carbon cloth EC-CC1-060T; SUS316L porous sheet and carbon paper 24AA	30, 60	H_2, 0.1	2	0.00132 and 0.00240	100–500 mA/cm^2	500 mA/cm^2 303K, 1MPa or 2MPa > 95%
HyEt Group (2017) [217]	No data	No data	No data	No data	No data	No data	No data	H_2, 0.1	70–100	1	No data	No data

Table 6 (continued)

Author and Ref. (year)	Membrane electrode assembly (MEA)						Operating conditions					Performance in EHC
	Membrane (thickness)	Electrodes (active area)	Proton conductivity (S/cm)	Back-diffusion	Mechanical strength	GDL	Temp (°C)	Gas composition and P_{in} (MPa)	P_{out} (MPa)	Flow (Nm^3/h)	Applied voltage or applied current density	
Choi et al. (2017) [92]	Ba ($Zr_{0.30}Ce_{0.54}Y_{0.15}Cu_{0.01}$) O_{3-d} (85 μm)	Sr-doped $LaVO_3$ and Cu and Y-doped Ba (Ce, Zr) O_3] (both 0.080 mm)	No data	No data	No data	No data	600, 700	Humidified 50% H_2 gas balanced with He; 10 sccm	No data	No data	1000 mA/cm^2	Faraday efficiency of 84%; Applied voltage: (1) 1.07 V, (2) 0.51 V
Greenway Energy (2017) [144]	NafionN212 (50 μm), N211 (25 μm) N115(125μm); PBI Film (70μm); Advent; Fumatech (53 μm)	No data (500 cm^2)	0.5–0.11, 0.1, 0.08, 0.1	No data	No data	No data	No data	No data	No data	No data	1000–4000 mA/cm^2	No data
Rico-Zavala et al. (2018) [130]	(1) SPEEK, (2) SPEEK(HNT), (3) SPEEK (PWA/HNT30)	Pt/C, Pt, 0.5 mg/cm^2, (25 cm^2)	(100% relative humidity): (1)0.01158, (2) 0.01967, (3)0.02037	No different pressure: (1) 2.25×10^{-9}mols^{-1} cm^{-2} (2) 5.0×10^{-10} mols^{-1} cm^{-2} (3) 1.0×10^{-9} mols^{-1} cm^{-2}	29 MPa	Sigracet SGL24-BC	30, 60, 80	Humidified H_2	No data	0.0156	400 mA/cm^2	Evaluation in area and volume swelling, water uptake, proton conductivity
MEMPHYS (2019) [21]	No data	No data	No data	No data	No data	No data	20–80	H_2 80%/ N_2 20% gas, H_2 50%/N_2 50% gas mixture, 0.105–10	20	H_2: 0.0188, N_2: 0.0047; H_2: 0.0188, N_2: 0.0188	No data	Compression of the purified H_2 up to 20 MPa
Giner ELX (2019) [219]	PFSA, BP-ArF4	No data (50–300 cm^2)	0.106	No data	Sealing140MPa	No data	No data	H_2, 0.1–10	87.5	5.5617	1000 mA/cm^2	At 35MPa $\leq$0.250 V, $\geq$1000 mA/cm^2
Toray Industries (2019) [85]	Nafion NRE212, Toray20 μm, 50 μm	Pt, A/C: 0.3mg/cm^2, 0.7mg/cm^2 (100cm^2)	80°C, 80%RH Nafion:0.11; Toray:0.22	0.5 MPa different pressure 80°C, 90%RH, Nafion:5.5×10^{-9} cm^2/s cmHg ,Toray: 5.7×10^{-10} cm^2/s cmHg	35 MPa	(1) 1.3mm thick, Porosity:31.9%,Size: 100μm,Lazer Microscope image:25μm; (2) 1.1 mm, 49.1%, 10 μm, 50 μm; (3) 0.58 mm, 67.2%, 20 μm, 20 μm; (4) 0.01–1 mm, 10–20%, 10 μm, etch hole	30–80	H_2	45–82	0.005, 0.5,5	No data	The power consumption: 40% less than that of the mechanical compressor (0.29 KWh/Nm^3) at 500 mA/cm^2
Pingitore et al. (2019) [220]	meta/para-PBI, para-PBI (104 μm,39 μm)	No data	>0.150	No data	The compressive creep compliance $<2\times10^{-6}$ Pa^{-1}	No data	160–200	Humidified H_2 and reformate test gas	No data	No data	200–1000 mA/cm^2	No data
Sdanghi et al. (2019) [206]	Nafion XL, Nafion 117 (30 μm, 175 mm)	No data (30 cm^2)	No data	2.53×10^{-7}	No data	Sigracet (240 mm), a gold-coated porous titanium (PTL) pore size: 5 mm and thickness: 1 mm	60	Humidified H_2 (0.1 MPa)	3.2	0.0026–0.0103	0–1000 mA/cm^2	14–56%

emphasized in which membrane segment designs are promising. As for high-pressure conditions in which membranes are sandwiched in the middle, the edges of membranes are subjected to stronger mechanical forces as compared with the middle and can break. Here, clamping systems for MEAs need to be carefully designed to avoid uneven mechanical compression based on force analysis. And equipped with locally strengthened segment-designed membranes, the reliability of membranes can be ensured with high-pressure difference loading. In practice, multi-stage compression is also promising for modularity, easiness in expansibility and so on.

2. The design of CLs in EHCs requires further attention in which well-designed CLs can reduce reaction times, improve overall efficiency and lower startup costs. In terms of costs, the development of non-Pt catalysts is also important in which the tailoring of catalyst morphology and the control of accessible active sites are required to achieve comparable activities to Pt catalysts. In addition, the design of high-pressure CLs is also important in which CLs need to maintain high specific surface areas and stable structures under high pressure in EHCs because catalyst particles can easily agglomerate under high pressures and CLs can drop off or crack. And although current research into pressure-resistant nanostructures for either PEMFCs or PEMWEs is rare, it should become a promising direction for EHCs. Moreover, the reduction of noble metal loading and the exploration of appropriate coating methods on CLs should be given more attention and the research of non-Pt catalysts is imperative in which overall costs can be substantially reduced. Furthermore, the performance and durability of EHC catalysts will require further attention.
3. The search for water management strategies in EHCs is vital. Unlike fuel cells and water electrolysis systems, EHCs do not involve water as a reactant or a product. Therefore, effective measurements to add water and maintain water in EHCs to achieve balance are required. And although many methods have been proposed to add water to EHCs, the easiest is to periodically add humidified hydrogen from the anode side. Water conduction models are also required to allow for the better understanding of EHCs in many conditions, especially for high-pressure conditions.

In general, the main barriers of EHCs for practical application and commercialization involve technical issues (low robustness, reliability and durability) and component costs. And although EHCs possess great potential and have attracted increasing attention, the determination of device durability, reliability and robustness remains difficult through the large amount of available experimental data. However, practical experimental testing remains the most effective approach to achieve incremental progress in the resolution of these issues. And due to the rapid development of fuel cells, corresponding technologies can potentially be applied to EHCs as well and in the foreseeable future, the issues of materials, chemistries and water management in EHCs will gradually be resolved. As for the commercialization of EHCs, it will depend on the research and development of overall hydrogen systems based on a future hydrogen economy that includes public acceptance and low overall costs. Ultimately, EHC technologies with superior, maintenance-free life cycles will become a compelling choice over existing solutions in the future.

Acknowledgements This work was supported by the National Key Research and Development Program of China (2017YFB0102701), Guangdong Innovative and Entrepreneurial Research Team Program (2016ZT06N500), Shenzhen Peacock Plan (KQTD2016022620054656), Shenzhen Key Laboratory project (ZDSYS201603311013489), Development and Reform Commission of Shenzhen Municipality 2017 (No. 1106), Shenzhen Clean Energy Research Institute (No. CERI-KY-2019-003) and Guangdong Provincial Key Laboratory of Energy Materials for Electric Power (2018B030322001).

References

1. Ellabban, O., Abu-Rub, H., Blaabjerg, F.: Renewable energy resources: current status, future prospects and their enabling technology. Renew. Sust. Energy Rev. **39**, 748–764 (2014). https://doi.org/10.1016/j.rser.2014.07.113
2. Sovacool, B.K.: The intermittency of wind, solar, and renewable electricity generators: technical barrier or rhetorical excuse. Util. Policy **17**, 288–296 (2009). https://doi.org/10.1016/j.jup.2008.07.001
3. Sheffield, J.W., Sheffield, C. (eds.): Assessment of Hydrogen Energy for Sustainable Development (NATO Science for Peace & Security Series C: Environmental Security), Springer, Netherlands (2007)
4. Deutschmann, O., Maier, L.I., Riedel, U., et al.: Hydrogen assisted catalytic combustion of methane on platinum. Catal. Today **59**, 141–150 (2000). https://doi.org/10.1016/S0920-5861(00)00279-0
5. Luo, Q., Gu, Q., Zhang, J.Y., et al.: Phase equilibria, crystal structure and hydriding/dehydriding mechanism of $Nd_4Mg_{80}Ni_8$ compound. Sci. Rep. **5**, 15385 (2015)

6. Nejat Veziroğlu, T.: Hydrogen technology for energy needs of human settlements. Int. J. Hydrog. Energy **12**, 99–129 (1987). https://doi.org/10.1016/0360-3199(87)90086-3
7. Barbir, F., Veziroğlu, T.N., Plass, H.J.: Environmental damage due to fossil fuels use. Int. J. Hydrog. Energy **15**, 739–749 (1990). https://doi.org/10.1016/0360-3199(90)90005-J
8. Thomas, G.: Overview of Storage Development DOE Hydrogen Program. Sandia National Laboratories, Albuquerque (2000)
9. Ling, C., Guo, T., Lu, W., et al.: Ultrahigh photosensitivity and detectivity of hydrogen-treated TiO_2 nanorod arrays/SiO_2/Si heterojunction broadband photodetectors and its mechanism. J. Mater. Chem. C **6**, 2319–2328 (2018)
10. Cano, Z., Banham, D., Ye, S., et al.: Batteries and fuel cells for emerging electric vehicle markets. Nat. Energy **3**, 279–289 (2018). https://doi.org/10.1038/s41560-018-0108-1
11. Holladay, J.D., Hu, J., King, D.L., et al.: An overview of hydrogen production technologies. Catal. Today **139**, 244–260 (2009). https://doi.org/10.1016/j.cattod.2008.08.039
12. Barthelemy, H., Weber, M., Barbier, F.: Hydrogen storage: recent improvements and industrial perspectives. Int. J. Hydrog. Energy **42**, 7254–7262 (2017). https://doi.org/10.1016/j.ijhydene.2016.03.178
13. Cardarelli, F.: Materials Handbook: A Concise Desktop Reference. Springer, Berlin (2018)
14. Wipke, K., Sprik, S., Kurtz, J., et al.: Contract No. DE-AC36-08GO28308 National Fuel Cell Electric Vehicle Learning Demonstration Final Report. Contract (2012)
15. Parks, G.: Hydrogen Station Compression, Storage, and Dispensing Technical Status and Costs Independent Review. National Renewable Energy Laboratory, Golden (2014)
16. Toghyani, S., Baniasadi, E., Afshari, E.: Performance analysis and comparative study of an anodic recirculation system based on electrochemical pump in proton exchange membrane fuel cell. Int. J. Hydrog. Energy **43**, 19691–19703 (2018). https://doi.org/10.1016/j.ijhydene.2018.08.194
17. Toghyani, S., Afshari, E., Baniasadi, E.: A parametric comparison of three fuel recirculation system in the closed loop fuel supply system of PEM fuel cell. Int. J. Hydrog. Energy **44**, 7518–7530 (2019). https://doi.org/10.1016/j.ijhydene.2019.01.260
18. Barbir, F., Görgün, H.: Electrochemical hydrogen pump for recirculation of hydrogen in a fuel cell stack. J. Appl. Electrochem. **37**, 359–365 (2007). https://doi.org/10.1007/s10800-006-9266-0
19. Tao, Y.: Electrochemical Compression with Ion Exchange Membranes for Air Conditioning, Refrigeration and Other Related Applications (2017). https://doi.org/10.13016/M2PV6B85W
20. Chen, W., Cameron, B., Zagarola, M., et al.: A high pressure ratio DC compressor for tactical cryocoolers. SPIE Proc. **9821**, 98210O (2016). https://doi.org/10.1117/12.2224731
21. Schorer, L., Schmitz, S., Weber, A.: Membrane based purification of hydrogen system (MEMPHYS). Int. J. Hydrog. Energy **44**, 12708–12714 (2019). https://doi.org/10.1016/j.ijhydene.2019.01.108
22. Lozada-Hidalgo, M., Zhang, S., Hu, S., et al.: Scalable and efficient separation of hydrogen isotopes using graphene-based electrochemical pumping. Nat. Commun. **8**, 15215 (2017)
23. Sdanghi, G., Maranzana, G., Celzard, A., et al.: Review of the current technologies and performances of hydrogen compression for stationary and automotive applications. Renew. Sust. Energy Rev. **102**, 150–170 (2019). https://doi.org/10.1016/j.rser.2018.11.028
24. Bloch, H.P., Hoefner, J.J.: Reciprocating Compressors, p. 389. Elsevier, Amsterdam (1996)
25. Almasi, A.: Latest practical notes and recent lessons learned on reciprocating compressors. Aust. J. Mech. Eng. **14**, 138–150 (2016). https://doi.org/10.1080/14484846.2015.1093681
26. Tuhovcak, J., Hejcik, J., Jicha, M.: Comparison of heat transfer models for reciprocating compressor. Appl. Therm. Eng. **103**, 607–615 (2016). https://doi.org/10.1016/j.applthermaleng.2016.04.120
27. Rahman, M.S.: Experimental and numerical study of snuber in hydrogen compressor. Int. J. Sci. Eng. **3**, 21–25 (2012)
28. Almasi, A.: Reciprocating compressor optimum design and manufacturing with respect to performance, reliability and cost. World Acad. Sci. Eng. Technol. **52**, 48–53 (2009)
29. Hitachi Infrastructure Systems (Asia) Pte. Ltd.: High-Pressure Hydrogen Compressors (100 MPa-Class Hydrogen Compressors for Hydrogen Refueling Stations) (2014).http://www.hitachi-infra.com.sg/services/_social_infrastructure_systems/compressor/reciprocating/hydrogen.html. Accessed 20 Jun 2020
30. Pirro, D.M., Daschner, E.: Lubrication Fundamentals. CRC Press, Boca Raton (2001)
31. Ahmed, S., Sutherland, E: 2013 Hydrogen Compression, Storage and Dispensing Cost Reduction Workshop Final Report. Argonne National Laboratory (2013)
32. Roy, A., Watson, S., Infield, D.: Comparison of electrical energy efficiency of atmospheric and high-pressure electrolysers. Int. J. Hydrog. Energy **31**, 1964–1979 (2006). https://doi.org/10.1016/j.ijhydene.2006.01.018
33. Jörissen, L.: Hydrogen and fuel cells. Fundamentals, technologies and applications. Edited by Detlev Stolten. Angew. Chem. Int. Ed. **50**, 9787 (2011). https://doi.org/10.1002/anie.201103583
34. Jiahao, C., Xiaohan, J., Chuang, X., et al.: Design and validation of new cavity profiles for diaphragm stress reduction in a diaphragm compressor. IOP Conf. Ser. Mater. Sci. Eng. (2015). https://doi.org/10.1088/1757-899X/90/1/012083
35. Jia, X., Zhao, Y., Chen, J., et al.: Research on the flowrate and diaphragm movement in a diaphragm compressor for a hydrogen refueling station. Int. J. Hydrog. Energy **41**, 14842–14851 (2016). https://doi.org/10.1016/j.ijhydene.2016.05.274
36. Li, J., Jia, X., Wu, Z., Peng, X.: The cavity profile of a diaphragm compressor for a hydrogen refueling station. Int. J. Hydrog. Energy **39**, 3926–3935 (2014). https://doi.org/10.1016/j.ijhydene.2013.12.152
37. Hofer - Neuman & Esser Group.: Hofer Diaphragm Compressors (2017). http://www.andreas-hofer.de/en/products/diaphragm-compressors/examples/. Accessed 10 Jun 2020
38. PDC Machines.: Diaphragm Compressors (2017). http://03d379a.netsolhost.com/TestSite/diaphragm-compressors/. Accessed 1 Jun 2020
39. Machines, P.: World's leading hydrogen gas compressors for refueling stations (2018). https://www.pdcmachines.com/wpcontent/uploads/2018/07/PDC_compressors_issuu.pdf
40. Karner, D., Francfort, J.: Arizona public service-alternative fuel (hydrogen) pilot plant design report. In: Citeseer (2003)
41. Rosi, N.L., Eckert, J., Eddaoudi, M., et al.: Hydrogen storage in microporous metal-organic frameworks. Science **300**, 1127–1129 (2003). https://doi.org/10.1126/science.1083440
42. Hilgers, C., Uerdingen, M., Wagner, M., et al.: Processing and/or Operating Machine Comprising an Ionic Liquid as the Operating Liquid. U.S. Pat. US 2008/0038123A1 (2018)
43. Kermani, N.A., Petrushina, I., Nikiforov, A., et al.: Corrosion behavior of construction materials for ionic liquid hydrogen compressor. Int. J. Hydrog. Energy **41**, 16688–16695 (2016). https://doi.org/10.1016/j.ijhydene.2016.06.221
44. Natesan N.: Fuel cell bus workshop-linde H_2 fueling. diamond bar, CA (2013). https://www.arb.ca.gov/msprog/bus/zbus/workshop/3d_Natesan.pdf. Accessed 30 Jun 2020
45. Weingärtner, H.: Understanding ionic liquids at the molecular level: facts, problems, and controversies. Angew. Chem. Int. Ed. **47**, 654–670 (2008). https://doi.org/10.1002/anie.200604951

46. Armand, M., Endres, F., MacFarlane, D.R., et al.: Ionic-liquid materials for the electrochemical challenges of the future. Nat. Mater. **8**, 621–629 (2009). https://doi.org/10.1038/nmat2448
47. Predel, T., Schlücker, E., Wasserscheid, P., et al.: Ionic liquids as operating fluids in high pressure applications. Chem. Eng. Technol. **30**, 1475–1480 (2007). https://doi.org/10.1002/ceat.200700276
48. Ven, J.D.V.D., Li, P.Y.: Liquid piston gas compression. Appl. Energy **86**, 2183–2191 (2009)
49. Kermani, N.A.: Design and Prototyping of an Ionic Liquid Piston Compressor as a New Generation of Compressors for Hydrogen Refueling Stations. Technical University of Denmark, Lyngby (2017)
50. Petitpas, G., Moreno-Blanco, J., Espinosa-Loza, F., et al.: Rapid high density cryogenic pressure vessel filling to 345 bar with a liquid hydrogen pump. Int. J. Hydrog. Energy **43**, 19547–19558 (2018). https://doi.org/10.1016/j.ijhydene.2018.08.139
51. Air Product: The Cryogenic Hydrogen Compressor System (2047). http://www.airproducts.com/~/media/downloads/h/hydrogen-support-microsite/en-cryogenic-hydrogen-compressorsystem.pdf?La=en. Accessed 1 Jun 2020
52. Ahluwalia, R.K., Hua, T.Q., Peng, J.K., et al.: Technical assessment of cryo-compressed hydrogen storage tank systems for automotive applications. Int. J. Hydrog. Energy **35**, 4171–4184 (2010). https://doi.org/10.1016/j.ijhydene.2010.02.074
53. Aceves, S.M., Petitpas, G., Espinosa-Loza, F., et al.: Safe, long range, inexpensive and rapidly refuelable hydrogen vehicles with cryogenic pressure vessels. Int. J. Hydrog. Energy **38**, 2480–2489 (2013). https://doi.org/10.1016/j.ijhydene.2012.11.123
54. Kunze, K., Kircher, O.: Cryo-compressed Hydrogen Storage. BMW Group. Cryogenic Cluster Day, Oxford (2012)
55. Hübert, T., Boon-Brett, L., Buttner, W.: Sensors for Safety and Process Control in Hydrogen Technologies. CRC Press, Boca Raton (2016)
56. Grasman, S.E.: Hydrogen Energy and Vehicle Systems. CRC Press, Boca Raton (2012)
57. Ahluwalia, R.K., Peng, J.K.: Automotive hydrogen storage system using cryo-adsorption on activated carbon. Int. J. Hydrog. Energy **34**, 5476–5487 (2009). https://doi.org/10.1016/j.ijhydene.2009.05.023
58. Fierro, V., Zhao, W., Izquierdo, M.T., et al.: Adsorption and compression contributions to hydrogen storage in activated anthracites. Int. J. Hydrog. Energy **35**, 9038–9045 (2010). https://doi.org/10.1016/j.ijhydene.2010.06.004
59. Li, Y., Yang, R.: Gas adsorption and storage in metal-organic framework MOF-177. Langmuir ACS J Surf Colloids **23**, 12937–12944 (2008). https://doi.org/10.1021/la702466d
60. Panella, B., Hirscher, M., Pütter, H., et al.: Hydrogen adsorption in metal-organic frameworks: Cu-MOFs and Zn-MOFs compared. Adv. Funct. Mater. **16**, 520–524 (2006). https://doi.org/10.1002/adfm.200500561
61. Swain, S., Ghosh, I.: Conceptual design analysis of a compressor-driven sorption cooling system. Int. J. Energy Res. **34**, 1016–1026 (2010). https://doi.org/10.1002/er.1618
62. Koley, S., Ghosh, I.: New technique for generating continuous sorption cooling in a single adsorbent column. Appl. Therm. Eng. **55**, 33–42 (2013). https://doi.org/10.1016/j.applthermaleng.2013.03.005
63. Luo, B.J., Wang, Z.L., Yan, T., et al.: A non-lumped dynamic simulation method of sorption compressor for sorption cryocooler. Cryogenics **58**, 14–19 (2013)
64. Panella, B., Hirscher, M., Roth, S., et al.: Hydrogen adsorption in different carbon nanostructures. Carbon **43**, 2209–2214 (2005)
65. Tong, L., Xiao, J., Cai, Y., et al.: Thermal effect and flow-through cooling of an adsorptive hydrogen delivery tank. Int. J. Hydrog. Energy **41**, 16094–16100 (2016)
66. Hermosilla-Lara, G., Momen, G., Marty, P.H., et al.: Hydrogen storage by adsorption on activated carbon: investigation of the thermal effects during the charging process. Int. J. Hydrog. Energy **32**, 1542–1553 (2007)
67. Richard, M.A., Cossement, D., Chandonia, P.A.: Preliminary evaluation of the performance of an adsorption-based hydrogen storage system. AIChE J. **8**, 2985–2996 (2009)
68. Srinivasa Murthy, S.: Heat and mass transfer in solid state hydrogen storage: a review. J. Heat Transf. (2012). https://doi.org/10.1115/1.4005156
69. Lototskyy, M.V., Yartys, V.A., Pollet, B.G., et al.: Metal hydride hydrogen compressors: a review. Int. J. Hydrog. Energy **39**, 5818–5851 (2014). https://doi.org/10.1016/j.ijhydene.2014.01.158
70. Dehouche, Z., Grimard, N., Laurencelle, F., et al.: Hydride alloys properties investigations for hydrogen sorption compressor. J. Alloys Compd. **399**, 224–236 (2005). https://doi.org/10.1016/j.jallcom.2005.01.029
71. Koultoukis, E., Makridis, S., Fruchart, D., et al.: Two-stage hydrogen compression using zr-based metal hydrides. Solid State Phenom. (2012). https://doi.org/10.4028/www.scientific.net/SSP.194.249
72. Hu, X.-C., Qi, Z.-G., Yang, M., et al.: A 38 MPa compressor based on metal hydrides. J. Shanghai Jiaotong Univ. (Sci.) **17**, 53–57 (2012). https://doi.org/10.1007/s12204-012-1229-5
73. Kelly, N.A., Girdwood, R.: Evaluation of a thermally-driven metal-hydride-based hydrogen compressor. Int. J. Hydrog. Energy **37**, 10898–10916 (2012). https://doi.org/10.1016/j.ijhydene.2012.04.088
74. Pickering, L., Reed, D., Bevan, A.I., et al.: Ti–V–Mn based metal hydrides for hydrogen compression applications. J. Alloys Compd. **645**, S400–S403 (2015). https://doi.org/10.1016/j.jallcom.2014.12.098
75. Rochlitz, L., Steinberger, M., Oechsner, R., et al.: Second use or recycling of hydrogen waste gas from the semiconductor industry—economic analysis and technical demonstration of possible pathways. Int. J. Hydrog. Energy **44**, 17168–17184 (2019). https://doi.org/10.1016/j.ijhydene.2019.05.009
76. Nowotny, J., Sorrell, C.C., Sheppard, L.R., et al.: Solar-hydrogen: environmentally safe fuel for the future. Int. J. Hydrog. Energy **30**, 521–544 (2005). https://doi.org/10.1016/j.ijhydene.2004.06.012
77. Schorer, L., Schmitz, S., Weber, A.: Membrane based purification of hydrogen system (MEMPHYS). Int. J. Hydrog. Energy (2019). https://doi.org/10.1016/j.ijhydene.2019.01.108
78. Nordio, M., Rizzi, F., Manzolini, G., et al.: Experimental and modelling study of an electrochemical hydrogen compressor. Chem. Eng. J. (2019). https://doi.org/10.1016/j.cej.2019.03.106
79. Corgnale, C., Sulic, M.: Techno-economic analysis of high-pressure metal hydride compression systems. Metals **8**, 469 (2018). https://doi.org/10.3390/met8060469
80. Corgnale, C., Greenway, S., Motyka, T., et al.: Technical performance of a hybrid thermo-electrochemical system for high pressure hydrogen compression. ECS Trans. **80**, 41–54 (2017)
81. Tao, Y., Lee, H., Hwang, Y., et al.: Electrochemical compressor driven metal hydride heat pump. Int. J. Refrig **60**, 278–288 (2015). https://doi.org/10.1016/j.ijrefrig.2015.08.018
82. Giner ELX, Inc.: 2019 Doe Hydrogen and Fuel Cells Program Annual Merit Review Meeting (2019)
83. Grigoriev, S.A., Shtatniy, I.G., Millet, P., et al.: Description and characterization of an electrochemical hydrogen compressor/concentrator based on solid polymer electrolyte technology. Int. J. Hydrog. Energy **36**, 4148–4155 (2011). https://doi.org/10.1016/j.ijhydene.2010.07.012
84. Bessarabov, D., Wang, H., Li, H., et al.: PEM Electrolysis for Hydrogen Production (Principles and Applications)||Generation

of Ozone and Hydrogen in a PEM Electrolyzer. CRC Press, Boca Raton (2015)
85. Toray Industries, Inc.: Research on Electrochemical Hydrogen Compressor. P13002, 20170000000203. NEDO Japan (2017)
86. Breiter, M.W.: Reaction Mechanisms of the H_2 Oxidation/Evolution Reaction. Wiley, New York (2010)
87. Chen, S., Kucernak, A.: Electrocatalysis under conditions of high mass transport: investigation of hydrogen oxidation on single submicron pt particles supported on carbon. J. Phys. Chem. B **108**, 13984–13994 (2004). https://doi.org/10.1021/jp048641u
88. Rico Zavala, A., Matera, F., Arjona, N., et al.: Nanocomposite membrane based on SPEEK as a perspectives application in electrochemical hydrogen compressor. Int. J. Hydrog. Energy **4**, 4 (2019). https://doi.org/10.1016/j.ijhydene.2018.12.174
89. Wu, X., He, G., Yu, L., et al.: Electrochemical hydrogen pump with SPEEK/CrPSSA semi-interpenetrating polymer network proton exchange membrane for H_2/CO_2 separation. ACS Sustain. Chem. Eng. **2**, 75–79 (2014). https://doi.org/10.1021/sc400329s
90. Rosli, R.E., Sulong, A.B., Daud, W.R.W., et al.: A review of high-temperature proton exchange membrane fuel cell (HT-PEMFC) system. Int. J. Hydrog. Energy **42**, 9293–9314 (2017). https://doi.org/10.1016/j.ijhydene.2016.06.211
91. Sakai, T., Isa, K., Matsuka, M., et al.: Electrochemical hydrogen pumps using Ba doped $LaYbO_3$ type proton conducting electrolyte. Int. J. Hydrog. Energy **38**, 6842–6847 (2013)
92. Choi, J., Shin, M., Kim, B., et al.: High-performance ceramic composite electrodes for electrochemical hydrogen pump using protonic ceramics. Int. J. Hydrog. Energy **42**, 13092–13098 (2017). https://doi.org/10.1016/j.ijhydene.2017.04.061
93. Kreuer, K.D.: Proton-conducting oxides. Annu. Rev. Mater. Res. **33**, 333–359 (2003). https://doi.org/10.1146/annurev.matsci.33.022802.091825
94. Kokkofitis, C., Ouzounidou, M., Skodra, A., et al.: High temperature proton conductors: applications in catalytic processes. Solid State Ionics **178**, 507–513 (2007). https://doi.org/10.1016/j.ssi.2006.11.010
95. Vasileiou, E., Kyriakou, V., Garagounis, I., et al.: Electrochemical enhancement of ammonia synthesis in a $BaZr_{0.7}Ce_{0.2}Y_{0.1}O_{2.9}$ solid electrolyte cell. Solid State Ionics **288**, 357–362 (2016). https://doi.org/10.1016/j.ssi.2015.12.022
96. Ulsh, M.: Membrane electrode assembly manufacturing automation technology for the electrochemical compression of hydrogen (2019). https://www.hydrogen.energy.gov/pdfs/review19/h2006_ulsh_2019_p.pdf
97. Barbir, F., Boston, A., London, H., et al.: PEM Fuel Cells: Theory and Practice. Academic Press, Cambridge (2005)
98. Stumper, J., Löhr, M., Hamada, S.: Diagnostic tools for liquid water in PEM fuel cells. J. Power Sources **143**, 150–157 (2005). https://doi.org/10.1016/j.jpowsour.2004.11.036
99. Knights, S.D., Colbow, K.M., St-Pierre, J., et al.: Aging mechanisms and lifetime of PEFC and DMFC. J. Power Sources **127**, 127–134 (2004). https://doi.org/10.1016/j.jpowsour.2003.09.033
100. Jung, A., Oh, J., Han, K., et al.: An experimental study on the hydrogen crossover in polymer electrolyte membrane fuel cells for various current densities. Appl. Energy **175**, 212–217 (2016). https://doi.org/10.1016/j.apenergy.2016.05.016
101. Cheng, X., Zhang, J., Tang, Y., et al.: Hydrogen crossover in high temperature PEM fuel cells. J. Power Sources (2007). https://doi.org/10.1016/j.jpowsour.2007.02.027
102. Zhang, J., Zhang, H., Wu, J., et al.: Chapter 6—hydrogen crossover. In: Zhang, J., Wu, J., Zhang, H. (eds.) PEM Fuel Cell Testing and Diagnosis, pp. 171–185. Newnes, Oxford (2013)
103. Truc, N.T., Ito, S., Fushinobu, K.: Numerical and experimental investigation on the reactant gas crossover in a PEM fuel cell. Int. J. Heat Mass Trans. **127**, 447–456 (2018). https://doi.org/10.1016/j.ijheatmasstransfer.2018.07.092
104. Kocha, S.S., Deliang Yang, J., Yi, J.S.: Characterization of gas crossover and its implications in PEM fuel cells. AIChE J. **52**, 1916–1925 (2006). https://doi.org/10.1002/aic.10780
105. Sompalli, B., Litteer, B., Gu, W., et al.: Membrane degradation at catalyst layer edges in PEMFC MEAs. J. Electrochem. Soc. **154**, B1349–B1357 (2007). https://doi.org/10.1149/1.2789791
106. Millet, P., Ngameni, R., Grigoriev, S.A., et al.: PEM water electrolyzers: from electrocatalysis to stack development. Int. J. Hydrog. Energy **35**, 5043–5052 (2010)
107. Lee, H.K., Choi, H.Y., Choi, K.H., et al.: Hydrogen separation using electrochemical method. J. Power Sources **132**, 92–98 (2004). https://doi.org/10.1016/j.jpowsour.2003.12.056
108. Abdulla, A., Laney, K., Padilla, M., et al.: Efficiency of hydrogen recovery from reformate with a polymer electrolyte hydrogen pump. AIChE J. **57**, 1767–1779 (2011). https://doi.org/10.1002/aic.12406
109. Catalano, J., Bentien, A., Østedgaard-Munck, D., et al.: Efficiency of electrochemical gas compression, pumping and power generation in membranes. J. Membr. Sci. **47**, 8 (2015). https://doi.org/10.1016/j.memsci.2014.12.042
110. Xuan, C., Zhang, J., Tang, Y., et al.: Hydrogen crossover in high-temperature PEM fuel cells. J. Power Sources **167**, 25–31 (2007)
111. Bloomfield, D.P., MacKenzie, B.S: Electrochemical Hydrogen Compressor. DOE US. (2006)
112. Ströbel, R., Oszcipok, M., Fasil, M., et al.: The compression of hydrogen in an electrochemical cell based on a PE fuel cell design. J. Power Sources **105**, 208–215 (2002). https://doi.org/10.1016/S0378-7753(01)00941-7
113. Sdanghi, G., Dillet, J., Didierjean, S., et al.: Feasibility of hydrogen compression in an electrochemical system: focus on water transport mechanisms. Fuel Cells **20**, 370–380 (2020)
114. Alvarez, A., Guzmán, C., Carbone, A., et al.: Composite membranes based on micro and mesostructured silica: a comparison of physicochemical and transport properties. J. Power Sources **196**, 5394–5401 (2011). https://doi.org/10.1016/j.jpowsour.2011.02.072
115. Saccà, A., Carbone, A., Gatto, I., et al.: Composites Nafion-titania membranes for polymer electrolyte fuel cell (PEFC) applications at low relative humidity levels: chemical physical properties and electrochemical performance. Polym. Test. **56**, 10–18 (2016). https://doi.org/10.1016/j.polymertesting.2016.09.015
116. Zhang, H., Ma, C., Wang, J., et al.: Enhancement of proton conductivity of polymer electrolyte membrane enabled by sulfonated nanotubes. Int. J. Hydrog. Energy **39**, 974–986 (2014). https://doi.org/10.1016/j.ijhydene.2013.10.145
117. Robert C. McDonald, S., Anthony B., LaConti, L.: Composite proton exchange membrane and method of manufacturing the same. US7326736B2 (2006)
118. Middelman, E.: High Differential Pressure Electrochemical Cell Comprising a Specific Membrane. EP2396458A1 (2010)
119. Kusoglu, A., Calabrese, M., Weber, A.: Effect of mechanical compression on chemical degradation of Nafion membranes. ECS Electrochem. Lett. **3**, F33–F36 (2014). https://doi.org/10.1149/2.008405eel
120. Yoon, W., Huang, X.: Acceleration of chemical degradation of perfluorosulfonic acid ionomer membrane by mechanical stress: experimental evidence. In: 218th ECS Meeting (2010)
121. Greenway Inc.: Hybrid Electrochemical Hydrogen/Metal Hydride Compression. DOE US (2018)
122. Bruijn, F., Dam, V.A., Janssen, G.: Review: durability and degradation issues of PEM fuel cell components. Fuel Cells **8**, 3–22 (2008). https://doi.org/10.1002/fuce.200700053
123. Nguyen, M.T., Grigoriev, S.A., Kalinnikov, A.A., et al.: Characterisation of a electrochemical hydrogen pump using electrochemical impedance spectroscopy. J. Appl. Electrochem. **41**, 1033 (2011). https://doi.org/10.1007/s10800-011-0341-9

124. Gardner, C.L., Ternan, M.: Electrochemical separation of hydrogen from reformate using PEM fuel cell technology. J. Power Sources **171**, 835–841 (2007). https://doi.org/10.1016/j.jpowsour.2007.06.020
125. Casati, C., Longhi, P., Zanderighi, L., et al.: Some fundamental aspects in electrochemical hydrogen purification/compression. J. Power Sources **180**, 103–113 (2008). https://doi.org/10.1016/j.jpowsour.2008.01.096
126. Attaran, A.M., Javanbakht, M., Hooshyari, K., et al.: New proton conducting nanocomposite membranes based on poly vinyl alcohol/poly vinyl pyrrolidone/$BaZrO_3$ for proton exchange membrane fuel cells. Solid State Ionics **269**, 98–105 (2015). https://doi.org/10.1016/j.ssi.2014.11.003
127. Mollá, S., Compañ, V.: Polymer blends of SPEEK for DMFC application at intermediate temperatures. Int. J. Hydrog. Energy **39**, 5121–5136 (2014). https://doi.org/10.1016/j.ijhydene.2014.01.085
128. Zhong, S., Cui, X., Cai, H., et al.: Crosslinked sulfonated poly(ether ether ketone) proton exchange membranes for direct methanol fuel cell applications. J. Power Sources **164**, 65–72 (2007). https://doi.org/10.1016/j.jpowsour.2006.10.077
129. Sasikala, S., Sundarraman, M., Bhat, S.D., et al.: Functionalized bentonite clay-sPEEK based composite membranes for direct methanol fuel cells. Electrochim. Acta **135**, 232–241 (2014). https://doi.org/10.1016/j.electacta.2014.04.180
130. Rico-Zavala, A., Gurrola, M.P., Arriaga, L.G., et al.: Synthesis and characterization of composite membranes modified with Halloysite nanotubes and phosphotungstic acid for electrochemical hydrogen pumps. Renew. Energy **122**, 163–172 (2018). https://doi.org/10.1016/j.renene.2018.01.054
131. Greenway Energy, Inc.: III.12 Hybrid Electrochemical Hydrogen/Metal Hydride Compressor. DOE US (2017)
132. Hamdan, M.: III.11 Electrochemical Compression. DOE US (2017)
133. Yang, B., Manohar, A., Prakash, G.K.S., Chen, W., Narayanan, S.R.: Anhydrous proton-conducting membrane based on poly-2-vinylpyridinium dihydrogenphosphate for electrochemical applications. J. Phys. Chem. B **115**, 14462–14468 (2011). https://doi.org/10.1021/jp206774c
134. Molter T. Development of an Electrochemical Separator and Compressor (2011)
135. Lipp, L.: Electrochemical Hydrogen Compressor. DOE US (2014)
136. Maiti, J., Kakati, N., Woo, S.P., et al.: Nafion® based hybrid composite membrane containing GO and dihydrogen phosphate functionalized ionic liquid for high temperature polymer electrolyte membrane fuel cell. Compos. Sci. Technol. **155**, 189–196 (2018). https://doi.org/10.1016/j.compscitech.2017.11.030
137. Yin, Y., Li, Z., Yang, X., et al.: Enhanced proton conductivity of Nafion composite membrane by incorporating phosphoric acid-loaded covalent organic framework. J. Power Sources **332**, 265–273 (2016). https://doi.org/10.1016/j.jpowsour.2016.09.135
138. Kim, S.J., Lee, B.S., Sang, H.A., et al.: Characterizations of polybenzimidazole based electrochemical hydrogen pumps with various Pt loadings for H_2/CO_2 gas separation. Int. J. Hydrog. Energy **38**, 14816–14823 (2013)
139. Perry, K., Eisman, G., Benicewicz, B.: Electrochemical hydrogen pumping using a high-temperature polybenzimidazole (PBI) membrane. J. Power Sources **177**, 478–484 (2008). https://doi.org/10.1016/j.jpowsour.2007.11.059
140. Onda, K., Ichihara, K., Nagahama, M., et al.: Separation and compression characteristics of hydrogen by use of proton exchange membrane. J. Power Sources **164**, 1–8 (2007). https://doi.org/10.1016/j.jpowsour.2006.10.018
141. Thomassen, M., Sheridan, E., Kvello, J.: Electrochemical hydrogen separation and compression using polybenzimidazole (PBI) fuel cell technology. J. Nat. Gas Sci. Eng. **2**, 229–234 (2010). https://doi.org/10.1016/j.jngse.2010.10.002
142. Buelte, S., Lewis, D., Eisman, G.: Effects of phosphoric acid concentration on platinum catalyst and phosphoric acid hydrogen pump performance. ECS Trans. **41**, 1955 (2011)
143. Pingitore, A., Huang, F., Qian, G., et al.: Durable high polymer content m/p -polybenzimidazole membranes for extended lifetime electrochemical devices. ACS Appl. Energy Mater. (2019). https://doi.org/10.1021/acsaem.8b01820
144. Yang, T., Chung, T.S.: High performance ZIF-8/PBI nano-composite membranes for high temperature hydrogen separation consisting of carbon monoxide and water vapor. Int. J. Hydrog. Energy **38**, 229–239 (2013). https://doi.org/10.1016/j.ijhydene.2012.10.045
145. Glenn Eisman (Primary Contact), D.S., Chuck Carlstrom: II.C.2 Process Intensification of Hydrogen Unit Operations Using an Electrochemical Device. DOE US (2012)
146. Sedlak, J.M., Austin, J.F., LaConti, A.B.: Hydrogen recovery and purification using the solid polymer electrolyte electrolysis cell. Int. J. Hydrog. Energy **6**, 45–51 (1981). https://doi.org/10.1016/0360-3199(81)90096-3
147. Hao, Y., Nakajima, H., Yoshizumi, H., et al.: Characterization of an electrochemical hydrogen pump with internal humidifier and dead-end anode channel. Int. J. Hydrog. Energy **41**, 13879–13887 (2016)
148. Lubers, A.M., Drake, A.W., Ludlow, D.J., et al.: Electrochemical hydrogen pumping using a platinum catalyst made in a fluidized bed via atomic layer deposition. Powder Technol. **296**, 72–78 (2015). https://doi.org/10.1016/j.powtec.2015.08.014
149. Moton, J.M., James, B.D., Colella, W.G.: Advances in electrochemical compression of hydrogen. In: ASME 2014 12th International Conference on Fuel Cell Science, Engineering and Technology Collocated with the ASME 2014 8th International Conference on Energy Sustainability, p. V001T01A002 (2014)
150. Alia, S., Pylypenko, S., Neyerlin, K., et al.: Activity and durability of iridium nanoparticles in the oxygen evolution reaction. ECS Trans. **69**, 883–892 (2015). https://doi.org/10.1149/06917.0883ecst
151. Spöri, C., Kwan, J.T.H., Bonakdarpour, A., et al.: The stability challenges of oxygen evolving catalysts: towards a common fundamental understanding and mitigation of catalyst degradation. Angew. Chem. Int. Ed. **56**, 5994–6021 (2017). https://doi.org/10.1002/anie.201608601
152. Mohammadi Taghiabadi, M., Zhiani, M.: Degradation analysis of dead-ended anode PEM fuel cell at the low and high thermal and pressure conditions. Int. J. Hydrog. Energy **44**, 4985–4995 (2019). https://doi.org/10.1016/j.ijhydene.2019.01.040
153. Kim, O.H., Cho, Y.H., Kang, S., et al.: Ordered macroporous platinum electrode and enhanced mass transfer in fuel cells using inverse opal structure. Nat. Commun. **4**, 2473 (2013). https://doi.org/10.1038/ncomms3473
154. Taylor, A.D., Kim, E.Y., Humes, V.P., et al.: Inkjet printing of carbon supported platinum 3-D catalyst layers for use in fuel cells. J. Power Sources **171**, 101–106 (2007). https://doi.org/10.1016/j.jpowsour.2007.01.024
155. Debe, M.K., Schmoeckel, A.K., Vernstrom, G.D., et al.: High voltage stability of nanostructured thin film catalysts for PEM fuel cells. J. Power Sources **161**, 1002–1011 (2006). https://doi.org/10.1016/j.jpowsour.2006.05.033
156. Kongkanand, A., Dioguardi, M., Ji, C., et al.: Improving operational robustness of NSTF electrodes in PEM fuel cells. J. Electrochem. Soc. **159**, F405–F411 (2012). https://doi.org/10.1149/2.045208jes
157. Jang, S., Kim, S., Kim, S.M., et al.: Interface engineering for high-performance direct methanol fuel cells using multiscale patterned membranes and guided metal cracked layers. Nano

Energy **43**, 149–158 (2018). https://doi.org/10.1016/j.nanoen.2017.11.011
158. Malevich, D., Saha, M., Halliop, E., et al.: Performance characteristics of PEFCs with patterned electrodes prepared by piezoelectric printing. ECS Trans. **50**, 423–427 (2013). https://doi.org/10.1149/05002.0423ecst
159. Lee, D.-H., Jo, W., Yuk, S., et al.: In-plane channel-structured catalyst layer for polymer electrolyte membrane fuel cells. ACS Appl. Mater. Interfaces **10**, 4682–4688 (2018). https://doi.org/10.1021/acsami.7b16433
160. Zhang, Z., Liu, J., Gu, J., et al.: An overview of metal oxide materials as electrocatalysts and supports for polymer electrolyte fuel cells. Energy Environ. Sci. (2014). https://doi.org/10.1039/C3EE43886D
161. Ganesan, A., Narayanasamy, M., Shunmugavel, K.: Self-humidifying manganese oxide-supported Pt electrocatalysts for highly-durable PEM fuel cells. Electrochim. Acta **285**, 47–59 (2018). https://doi.org/10.1016/j.electacta.2018.08.001
162. Tokarev, A., Bessarabov, D.G.: Modeling of bimetallic Pt-based electrocatalyst on extended-surface support for advanced hydrogen compression and separation. Int. J. Hydrog. Energy **39**, 7805–7810 (2014). https://doi.org/10.1016/j.ijhydene.2014.03.138
163. Kim, S.J., Park, H.Y., Ahn, S.H., et al.: Highly active and CO_2 tolerant Ir nanocatalysts for H_2/CO_2 separation in electrochemical hydrogen pumps. Appl. Catal. B Environ. **158–159**, 348–354 (2014). https://doi.org/10.1016/j.apcatb.2014.04.016
164. Zheng, Y., Jiao, Y., Jaroniec, M., et al.: Advancing the electrochemistry of the hydrogen-evolution reaction through combining experiment and theory. Angew. Chem. Int. Ed. **54**, 52–65 (2015). https://doi.org/10.1002/anie.201407031
165. Zheng, Y., Jiao, Y., Zhu, Y., et al.: Hydrogen evolution by a metal-free electrocatalyst. Nat. Commun. **5**, 3783 (2014). https://doi.org/10.1038/ncomms4783
166. Zhang, J., Qu, L., Shi, G., et al.: N, P-codoped carbon networks as efficient metal-free bifunctional catalysts for oxygen reduction and hydrogen evolution reactions. Angew. Chem. Int. Ed. **55**, 2230–2234 (2016). https://doi.org/10.1002/anie.201510495
167. Yu, X.-Y., Feng, Y., Jeon, Y., et al.: Formation of Ni–Co–MoS_2 Nanoboxes with enhanced electrocatalytic activity for hydrogen evolution. Adv. Mater. **28**, 9006–9011 (2016). https://doi.org/10.1002/adma.201601188
168. Cao, B., Veith, G.M., Neuefeind, J.C., et al.: Mixed close-packed cobalt molybdenum nitrides as non-noble metal electrocatalysts for the hydrogen evolution reaction. J. Am. Chem. Soc. **135**, 19186–19192 (2013). https://doi.org/10.1021/ja4081056
169. Bukola, S., Cao, D., Martinson, A.B.F., et al.: Effects of atomic-layer-deposition alumina on proton transmission through single-layer graphene in electrochemical hydrogen pump cells. ACS Appl. Energy Mater. **3**, 1364–1372 (2020). https://doi.org/10.1021/acsaem.9b01775
170. Yu, W., Porosoff, M.D., Chen, J.G.: Review of Pt-based bimetallic catalysis: from model surfaces to supported catalysts. Chem. Rev. **112**, 5780–5817 (2012). https://doi.org/10.1021/cr300096b
171. Li, C., Baek, J.-B.: Recent advances in noble metal (Pt, Ru, and Ir)-based electrocatalysts for efficient hydrogen evolution reaction. ACS Omega **5**, 31–40 (2020). https://doi.org/10.1021/acsomega.9b03550
172. Hinnemann, B., Moses, P.G., Bonde, J., et al.: Biomimetic hydrogen evolution: MoS2 nanoparticles as catalyst for hydrogen evolution. J. Am. Chem. Soc. **127**, 5308–5309 (2005). https://doi.org/10.1021/ja0504690
173. Ambrosi, A., Sofer, Z., Pumera, M.: Molybdenum disulfide: lithium intercalation compound dramatically influences the electrochemical properties of exfoliated MoS_2. Small **11**, 604 (2015). https://doi.org/10.1002/smll.201570030
174. Choi, C.L., Feng, J., Li, Y., et al.: WS_2 nanoflakes from nanotubes for electrocatalysis. Nano Res. **6**, 921–928 (2013). https://doi.org/10.1007/s12274-013-0369-8
175. Tan, Y., Liu, P., Chen, L., et al.: Monolayer MoS_2 films supported by 3D nanoporous metals for high-efficiency electrocatalytic hydrogen production. Adv. Mater. **26**, 8023–8028 (2014). https://doi.org/10.1002/adma.201403808
176. Oyama, S.T., Gott, T., Zhao, H., et al.: Transition metal phosphide hydroprocessing catalysts: a review. Catal. Today **143**, 94–107 (2009). https://doi.org/10.1016/j.cattod.2008.09.019
177. Kucernak, A.R.J., Naranammalpuram Sundaram, V.N.: Nickel phosphide: the effect of phosphorus content on hydrogen evolution activity and corrosion resistance in acidic medium. J. Mater. Chem. A **2**, 17435–17445 (2014)
178. Jiang, P., Liu, Q., Sun, X.: NiP_2 nanosheet arrays supported on carbon cloth: an efficient 3D hydrogen evolution cathode in both acidic and alkaline solutions. Nanoscale (2014). https://doi.org/10.1039/C4NR04866K
179. Jin, Z., Li, P., Huang, X., et al.: Three-dimensional amorphous tungsten-doped nickel phosphide microsphere as an efficient electrocatalyst for hydrogen evolution. J. Mater. Chem. A **2**, 18593–18599 (2014)
180. Huang, Z., Chen, Z., Chen, Z., et al.: Cobalt phosphide nanorods as an efficient electrocatalyst for the hydrogen evolution reaction. Nano Energy **9**, 373–382 (2014). https://doi.org/10.1016/j.nanoen.2014.08.013
181. Jiang, P., Liu, Q., Liang, Y., et al.: A cost-effective 3D hydrogen evolution cathode with high catalytic activity: FeP nanowire array as the active phase. Angew. Chem. Int. Ed. **53**, 12855–12859 (2014). https://doi.org/10.1002/anie.201406848
182. Xing, Z., Liu, Q., Asiri, A.M., et al.: Closely interconnected network of molybdenum phosphide nanoparticles: a highly efficient electrocatalyst for generating hydrogen from water. Adv. Mater. **26**, 5702–5707 (2014). https://doi.org/10.1002/adma.201401692
183. Kibsgaard, J., Jaramillo, T.F.: Molybdenum phosphosulfide: an active, acid-stable, earth-abundant catalyst for the hydrogen evolution reaction. Angew. Chem. Int. Ed. **53**, 14433–14437 (2014). https://doi.org/10.1002/anie.201408222
184. Chen, W.-F., Sasaki, K., Ma, C., et al.: Hydrogen-evolution catalysts based on non-noble metal nickel-molybdenum nitride nanosheets. Angew. Chem. Int. Ed. **51**, 6131–6135 (2012). https://doi.org/10.1002/anie.201200699
185. Hunt, S.T., Nimmanwudipong, T., Román-Leshkov, Y.: Engineering non-sintered, metal-terminated tungsten carbide nanoparticles for catalysis. Angew. Chem. Int. Ed. **53**, 5131–5136 (2014). https://doi.org/10.1002/anie.201400294
186. Kong, D., Wang, H., Cha, J.J., et al.: Synthesis of MoS_2 and $MoSe_2$ films with vertically aligned layers. Nano Lett. **13**, 1341–1347 (2013)
187. Onda, K., Araki, T., Ichihara, K., et al.: Treatment of low concentration hydrogen by electrochemical pump or proton exchange membrane fuel cell. J. Power Sources **188**, 1–7 (2009)
188. Shimpalee, S., Van Zee, J.W.: Numerical studies on rib and channel dimension of flow-field on PEMFC performance. Int. J. Hydrog. Energy **32**, 842–856 (2007). https://doi.org/10.1016/j.ijhydene.2006.11.032

189. Kahraman, H., Orhan, M.F.: Flow field bipolar plates in a proton exchange membrane fuel cell: analysis and modeling. Energy Convers. Manag. **133**, 363–384 (2017). https://doi.org/10.1016/j.enconman.2016.10.053
190. Wang, Q., Eikerling, M., Song, D., Liu, Z.-S., Navessin, T., Xie, Z., Holdcroft, S.: Functionally graded cathode catalyst layers for polymer electrolyte fuel cells. J. Electrochem. Soc. **151**, A1171 (2004). https://doi.org/10.1149/1.1753580
191. Himanen, O., Hottinen, T., Mikkola, M., et al.: Characterization of membrane electrode assembly with hydrogen-hydrogen cell and ac-impedance spectroscopy: part I. Experimental. Electrochim. Acta **52**, 206–214 (2006)
192. Lee, M., Huang, X.: Development of a hydrophobic coating for the porous gas diffusion layer in a PEM-based electrochemical hydrogen pump to mitigate anode flooding. Electrochem. Commun. **100**, 39–42 (2019). https://doi.org/10.1016/j.elecom.2019.01.017
193. Hao, Y.M., Nakajima, H., Inada, A., et al.: Overpotentials and reaction mechanism in electrochemical hydrogen pumps. Electrochim. Acta **301**, 274–283 (2019). https://doi.org/10.1016/j.electacta.2019.01.108
194. Qiu, D., Janßen, H., Peng, L., et al.: Electrical resistance and microstructure of typical gas diffusion layers for proton exchange membrane fuel cell under compression. Appl. Energy **231**, 127–137 (2018). https://doi.org/10.1016/j.apenergy.2018.09.117
195. Blanchet, E.D.S.: Resilient Flow Structures for Electrochemical Cell. U.S. Pat. US10305124B2 (2017)
196. Nitta, I., Hottinen, T., Himanen, O., et al.: Inhomogeneous compression of PEMFC gas diffusion layer: part I. Experimental. J. Power Sources **171**, 26–36 (2007). https://doi.org/10.1016/j.jpowsour.2006.11.018
197. Zhou, Y., Lin, G., Shih, A.J., et al.: Multiphysics modeling of assembly pressure effects on proton exchange membrane fuel cell performance. J. Fuel Cell Sci. Technol. (2009). https://doi.org/10.1115/1.3081426
198. Shi, Z., Wang, X., Guessous, L.: Effect of compression on the water management of a proton exchange membrane fuel cell with different gas diffusion layers. J. Fuel Cell Sci. Technol. (2010). https://doi.org/10.1115/1.3177451
199. Ge, J., Higier, A., Liu, H.: Effect of gas diffusion layer compression on PEM fuel cell performance. J. Power Sources **159**, 922–927 (2006). https://doi.org/10.1016/j.jpowsour.2005.11.069
200. LaConti, A.B., Titterington, W.A., Swette, L.L., et al.: Proton Exchange Membrane (PEM) Electrochemical Cell Having an Integral, Electrically-Conductive, Resiliently Compressible, Porous Pad. U.S. Pat. US7438985B2 (2008)
201. Lipp, L.: Electrochemical Hydrogen Compressor. DOE US (2016)
202. Yi, J.S.: An along-the-channel model for proton exchange membrane fuel cells. J. Electrochem. Soc. **145**, 1149 (1998). https://doi.org/10.1149/1.1838431
203. Berg, P., Promislow, K., St. Pierre, J., et al.: Water management in PEM fuel cells. J. Electrochem. Soc. **151**, A341 (2004). https://doi.org/10.1149/1.1641033
204. Misran, E., Hassan, N.S.M., Daud, W.R.W., et al.: Water transport characteristics of a PEM fuel cell at various operating pressures and temperatures. Int. J. Hydrog. Energy **38**, 9401–9408 (2013). https://doi.org/10.1016/j.ijhydene.2012.12.076
205. Kusoglu, A., Kienitz, B.L., Weber, A.Z.: Understanding the effects of compression and constraints on water uptake of fuel-cell membranes. J. Electrochem. Soc. **158**, B1504 (2011). https://doi.org/10.1149/2.097112jes
206. Sdanghi, G., Dillet, J., Didierjean, S., et al.: Feasibility of hydrogen compression in an electrochemical system: focus on water transport mechanisms. Fuel Cells (2019). https://doi.org/10.1002/fuce.201900068
207. Yanming, H.: Characterization of the Overpotential in Electrochemical Hydrogen Compressor with the Internal Humidifier and Anode Dead End Channel (2016)
208. Sdanghi, G., Dillet, J., Didierjean, S., et al.: Operating heterogeneities in a PEM electrochemical hydrogen compressor. Paper Presented at the 8th International Conference on Fundamentals and Development of Fuel Cells (2019). Nantes, France, 2019-02-12
209. Sdanghi, G., Dillet, J., Didierjean, S., et al.: Experimental evidence of local heterogeneities in a PEM electrochemical hydrogen compressor. Paper Presented at the European Fuel Cells Forum 2019, Lucerne, France, 2019-07-02
210. Bampaou, M.E.A.: An electrochemical hydrogen compression model. Chem. Eng. Trans. (2018). https://doi.org/10.3303/CET1870203
211. Rahbari, A., Brenkman, J., Hens, R., et al.: Solubility of water in hydrogen at high pressures: a molecular simulation study. J. Chem. Eng. Data **64**, 4103–4115 (2019). https://doi.org/10.1021/acs.jced.9b00513
212. Rohland, B., Eberle, K., Ströbel, R., et al.: Electrochemical hydrogen compressor. Electrochim. Acta **43**, 3841–3846 (1998). https://doi.org/10.1016/S0013-4686(98)00144-3
213. Ibeh, B., Gardner, C., Ternan, M.: Separation of hydrogen from a hydrogen/methane mixture using a PEM fuel cell. Int. J. Hydrog. Energy **32**, 908–914 (2007). https://doi.org/10.1016/j.ijhydene.2006.11.017
214. Dale, N., Biaku, C., Mann, M., et al.: Electrochemical compression of product hydrogen from PEM electrolyzer stack. In: NHA Annual Hydrogen Conference (2007)
215. Wu, X., He, G., Yu, L., et al.: Electrochemical hydrogen pump with SPEEK/CrPSSA semi-interpenetrating polymer network proton exchange membrane for H_2/CO_2 separation. ACS Sustain. Chem. Eng. **2**, 75–79 (2013)
216. Moton, J.M., James, B.D., Colella, W.G.: Advances in Electrochemical Compression of Hydrogen. 45882, V001T001A002 (2014). https://doi.org/10.1115/fuelcell2014-6641
217. Bouwman, P.J., Konink, J., Semerel, D., et al.: (Invited) Electrochemical hydrogen compression. ECS Trans. **64**, 1009 (2014)
218. Huang, S., Wang, T., Wu, X., et al.: Coupling hydrogen separation with butanone hydrogenation in an electrochemical hydrogen pump with sulfonated poly (phthalazinone ether sulfone ketone) membrane. J. Power Sources **327**, 178–186 (2016)
219. Giner ELX, Inc.: 2019 DOE hydrogen and fuel cells program. Annual Merit Review Meeting, April 29, Crystal City, Virginia, USA (2019)
220. Pingitore, A.T., Huang, F., Qian, G., et al.: Durable high polymer content m/p-polybenzimidazole membranes for extended lifetime electrochemical devices. ACS Appl. Energy Mater. **2**, 1720–1726 (2019). https://doi.org/10.1021/acsaem.8b01820

Jiexin Zou is currently a joint Ph.D. student between the Harbin Institute of Technology and the Southern University of Science and Technology under the supervision of Prof. Haijiang Wang. She received her B.S. in Engineering from Northeast Agricultural University (2018). Her research is focused on the optimization and design of electrochemical hydrogen compressor.

Ning Han is a Ph.D. candidate at Katholieke Universiteit Leuven, and a visiting scholar at Southern University of Science and Technology. His current research is mainly lie in design and characterization of oxide-based materials with the application focus on catalytic oxidation, electrocatalysis, and energy storage.

Jiangyan Yan is currently a postdoctoral researcher in Southern University of Science and Technology. She received her bachelor degree from Shandong Agriculture University in 2012 and Ph.D degree from North China Electric Power University in 2018. Her research is focused on the PEMFC system simulation and optimization.

Qi Feng obtained his Ph.D. degree in Harbin Institute of Technology on July 2020. His research is focused on hydrogen production and catalyst design.

Yajun Wang is currently a joint Ph.D. student between the Harbin Institute of Technology and the Southern University of Science and Technology under the supervision of Prof. Haijiang Wang. His research is focused on the optimization and design of proton exchange membrane fuel cell.

Zhiliang Zhao received his B.S. in Central South University in 2011 and Ph.D. in 2018 from the Southwest University. Now he is a postdoctor in Professor Hui Li's group at SUSTech. His research interests focus on advanced nanomaterials for electrochemical applications such as electrocatalysis, energy storage and conversion.

Jiantao Fan, ethnic Han, member of CPC. Vice President of "Shenzhen Hydrogen and Fuel Cell Association". Core member of "Guangdong Innovative and Entrepreneurial Research Team Program". Core member of "Shenzhen Peacock Plan". Class-C of "Shenzhen overseas high-level talents Program" (Peacock Plan Class-C). Project leader of 2019 national Key R&D program. Graduated from Beijing University of Chemical Technology at 2014. Post-doctoral research fellow in Simon Fraser University from 2014 to 2017. Focused on polyelectrolyte membrane and membrane electrode assembly study from 2009. At present, more than 20 academic papers have been published in academic journals such as Nature Communications, Energy & Environmental Science, ACS Macro Letters, Journal of Materials Chemistry A.

Lin Zeng research mainly involves the critical materials and the mass transfer mechanism at the solid/liquid interface for electrochemical energy systems, including fuel cells, water splitting and secondary batteries. Professor Zeng has published more than 50 papers in top-rated journals, including *Energy and Environmental Science*, *Nano Energy*, *Applied Energy*, *Journal of Power Sources*. According to Web of Science, his papers have been cited more than 1000 times with an H-index of 23.

Hui Li Chair Professor, joined the Department of Materials Science and Engineering at the Southern University of Science and Technology of China in October 2015. Prof. Li received her B.S. and M.Sc. in Chemical Engineering from Tsinghua University (China), and her Ph.D in Electrochemical Engineering from the University of British Columbia (Canada). She has over 20 years' experiences working on theoretical and applied electrochemistry and electrochemical engineering. Most notably, she worked for 8 years at the Institute for Fuel Cell Innovation of National Research Council of Canada as a research officer and Energy Storage Program technical leader. She has accumulated extensive experiences in PEM fuel cells and PEM water electrolysis-related areas. She was sitting in the ISO/WG14 group developing specs for air and hydrogen feeds for stationary FC applications. She authored 50 peer-reviewed journal papers and edited four books in the area of PEM fuel cells and electrolysis. Her two most recent review papers related to PEM fuel cell catalysts, one published in *Chemical Reviews* (2015) and the other in *Progress in Materials Science* (2016), are highly regarded in the PEM fuel cell catalyst development. Her current research topics mainly focus on PEM fuel cell key technologies and materials that hinder the large-scale commercialization and hydrogen production technologies.

Dr. Haijiang Wang has involved in the research sphere of fuel cells and their key components for more than 20 years. He is well-known as a fellow of the Canadian Academy of Engineering, the Chairman of Shenzhen SouthernTech Fuel Cell Corp., Inc. Dr. Wang joined the Southern University of Science and Technology in October, 2015. Dr. Wang has co-authored more than 200 research papers published in referred journals. His SCI papers are cited for more than 17,000 times, and the H factor is 54. In addition, Dr. Wang has also been granted 5 international patents and co-edited 15 books related to PEM fuel cells and PEM electrolyzers. Since 2014, Dr. Wang has been awarded as the most highly cited researchers for five consecutive years due to his impactful publications in fuel cell research by Thomson Reuters.